



Kinetic mechanisms by which nickel alters the calcium (Ca^{2+}) transport in intact rat liver

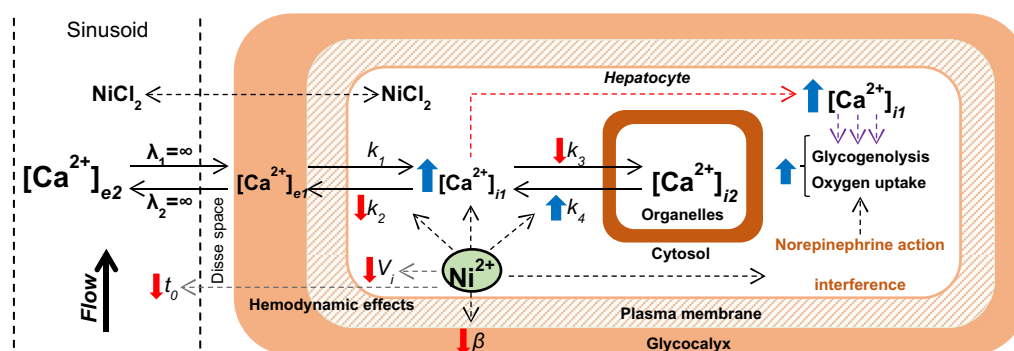
Karina Sayuri Utsunomiya¹ · Lucas Jonatas da Silva¹ · Juliana Iwamoto¹ · Rodrigo Polimeni Constantin¹ · Eduardo Hideo Gilgioni¹ · Jorgete Constantin¹ · Adelar Bracht¹ · Ronald Petrus Johannes Oude Elferink² · Emy Luiza Ishii-Iwamoto¹

Received: 13 May 2021 / Accepted: 14 July 2021 / Published online: 24 July 2021
© Society for Biological Inorganic Chemistry (SBIC) 2021

Abstract

In the present work, the multiple-indicator dilution (MID) technique was used to investigate the kinetic mechanisms by which nickel (Ni^{2+}) affects the calcium (Ca^{2+}) transport in intact rat liver. $^{45}\text{Ca}^{2+}$ and extra- and intracellular space indicators were injected in livers perfused with 1 mM Ni^{2+} , and the outflow profiles were analyzed by a mathematical model. For comparative purposes, the effects of norepinephrine were measured. The influence of Ni^{2+} on the cytosolic Ca^{2+} concentration ($[\text{Ca}^{2+}]_c$) in human hepatoma Huh7 cells and on liver glycogen catabolism, a biological response sensitive to cellular Ca^{2+} , was also evaluated. The estimated transfer coefficients of $^{45}\text{Ca}^{2+}$ transport indicated two mechanisms by which Ni^{2+} increases the $[\text{Ca}^{2+}]_c$ in liver under steady-state conditions: (1) an increase in the net efflux of Ca^{2+} from intracellular Ca^{2+} stores due to a stimulus of Ca^{2+} efflux to the cytosolic space along with a diminution of Ca^{2+} re-entry into the cellular Ca^{2+} stores; (2) a decrease in Ca^{2+} efflux from the cytosolic space to vascular space, minimizing Ca^{2+} loss. Glycogen catabolism activated by Ni^{2+} was transient contrasting with the sustained activation induced by norepinephrine. Ni^{2+} caused a partial reduction in the norepinephrine-induced stimulation in the $[\text{Ca}^{2+}]_c$ in Huh7 cells. Our data revealed that the kinetic parameters of Ca^{2+} transport modified by Ni^{2+} in intact liver are similar to those modified by norepinephrine in its first minutes of action, but the membrane receptors or Ca^{2+} transporters affected by Ni^{2+} seem to be distinct from those known to be modulated by norepinephrine.

Graphic abstract



Keywords Liver hemodynamic · Toxicity · Enzyme kinetics · Heavy metal · Ca^{2+} -sensing receptor

✉ Emy Luiza Ishii-Iwamoto
eliwamoto@uem.br

Extended author information available on the last page of the article

Introduction

Nickel (Ni) is a naturally occurring metal that exists in several mineral forms, present in all compartments of the environment as Ni²⁺-containing compounds and complexes [1]. Despite exerting a fundamental role on the activity of many essential metalloenzymes in plants, bacteria, archaea, and unicellular eukaryotes, there are no known Ni²⁺-dependent enzymes or cofactors for vertebrates [2]. In addition to its biological role, the unique Ni physical and chemical properties make this metal and its compounds appropriate materials for various industrial applications, such as the generation of stainless steel and other alloys and in the production of lithium batteries [2]. These industrial uses of Ni lead to the environmental release and pollution by Ni and its products. Humans and animals are exposed to Ni products primarily via inhalation, ingestion, and dermal absorption with higher exposition under occupational exposures of workers in Ni-using industries [2–4]. Several biological factors affect the bioavailability of heavy metals, including the mechanisms of sequestration and transport by organic binders such as proteins [5–7]. After entering the body, Ni products are distributed to all organs, primarily in the kidneys, liver, bones, and lungs and can be gradually retained in the body in a “nickel pool” [1, 3, 8]. Despite reports of the harmful effects of Ni in humans and animals [9], there is limited information on the serum levels of Ni compounds under toxic conditions. The most common adverse health effects in humans are allergic reactions, abnormal pulmonary functions, renal tubular necrosis, cardiovascular diseases [10, 11], cardiac and hepatic damage, anemia, eosinophilia, neurological disorders, and cancer [2, 8, 12–14].

Ni²⁺, similar to other tri- and divalent cations, such as gadolinium (Gd³⁺), lanthanide (La³⁺), yttrium (Y³⁺), and cadmium (Cd²⁺), shares chemical properties with divalent calcium (Ca²⁺), especially in ionic radii, co-ordination chemistry and preference for the oxygen donor groups. This factor provides the basis for some of its interference in biological systems [15, 16]. Ni²⁺-mediated cellular Ca²⁺ homeostasis disruption has been reported in many cell types, such as osteoclasts, hepatocytes, Leydig cells, and lung epithelial cells, with an elevated cytosolic Ca²⁺ concentration ([Ca²⁺]_c) as a common effect [17–19]. The mechanisms of this action in different cell types are not totally known; most suggestions have been based on the use of specific inhibitors. In Leydig cells, for example, one study proposed that Ni²⁺ activates a Ca²⁺ receptor that mobilizes intracellular Ca²⁺ stores through ryanodine receptors [17]. In human-cultured airway epithelial cells, Cortijo et al. [18] demonstrated that the transient increase in intracellular Ca²⁺ is suppressed by inhibition

of phospholipase C (PLC) or inositol-1,4,5-trisphosphate (IP₃) release as well as by NPS2390, an antagonist of the extracellular Ca²⁺-sensing receptor (CaSR). CaSR is a member of the G-protein-coupled receptor superfamily [20, 21], whose activation has been demonstrated to increase the cytosolic Ca²⁺ concentration ([Ca²⁺]_c) that arises from G_q-mediated PLC activation, triggering IP₃ formation. This receptor is expressed primarily in the parathyroid glands, but it is also expressed in breast, blood vessels, liver, and placenta [22].

In mammals, Ni—similar to other heavy metal ions absorbed from the diet—enters the portal circulation and is transported to the liver, an organ that plays a key role in regulating its plasma concentration [23]. Unlike other heavy metals, such as Cd²⁺ and Zn²⁺, Ni²⁺ uptake in hepatocytes is not an -SH carrier-mediated transport process [24]. The involvement of transport through Ca²⁺ channels has been suggested by the partial inhibition of Ni²⁺ uptake by nica-dipine or verapamil [25]. Calcium regulates important liver functions, including hormone-stimulated glucose production and bile salt secretion [26, 27]. Indeed, Ni²⁺ reportedly interferes with the effects of Ca²⁺-mobilizing hormones, such as vasopressin and adenosine triphosphate (ATP) [28, 29]. Hughes and Barritt [30] suggested a direct action of Ni²⁺ on Ca²⁺ influx into the liver based on the inhibition of vasopressin and angiotensin-stimulated Ca²⁺ inflow in isolated hepatocytes. In perfused rat liver, Ni²⁺ reduces extracellular Ca²⁺ uptake induced by Ca²⁺-mobilizing hormones, an effect also interpreted as being a Ni²⁺ inhibitory action on Ca²⁺ influx into hepatocytes [28]. In a study with primary cultivated hepatocytes loaded with Fura-2 AM, McNulty and Taylor [19] demonstrated that Ni²⁺ increases [Ca²⁺]_c from the mobilization of the same intracellular Ca²⁺ stores as those modulated by [Arg⁸]vasopressin. However, the authors did not find evidence that Ni²⁺ affects Ca²⁺ influx from the extracellular medium into hepatocytes. The effect of Ni²⁺ on the [Ca²⁺]_c was shown to be transient, minimally affected by the removal of extracellular Ca²⁺, and suppressed when the intracellular Ca²⁺ stores were depleted by thapsigargin [19]. The discrepancy regarding the Ni²⁺ mode of action on hepatocytes is probably due to different experimental conditions and methodologies used for Ca²⁺ flux measurements. In isolated hepatocytes, the uptake of Ca²⁺ was assessed by measuring ⁴⁵Ca²⁺ associated with cells [30], in cultivated hepatocytes the [Ca²⁺]_c was indicated by Fura-2 AM [19] and in perfused rat liver, Ca²⁺ influx and efflux were calculated from changes in the perfusate Ca²⁺ concentration with a selective Ca²⁺ electrode [28].

A variety of channels, transporters, and co-transporters located in the plasma membrane (PM), endoplasmic reticulum (ER), and mitochondrial membranes are involved in the distribution and movements of cellular Ca²⁺ in hepatocytes

[31, 32]. Although considerable knowledge on Ca^{2+} transport systems has been derived from studies using isolated hepatocytes, data on kinetics of Ca^{2+} movements in isolated hepatocytes do not represent the steady-state condition of an intact liver, mainly due to the loss of spatial distribution and polarity of hepatocytes in the liver architecture. Hepatocytes in an intact liver are distributed in at least three distinct functional regions: the basal or sinusoidal membrane facing blood in the sinusoids, the lateral membrane facing the intercellular space, and the canalicular membrane [33]. The measurement of Ca^{2+} fluxes and distribution in an intact liver can be done by means of the multiple-indicator dilution (MID) technique. We successfully employed this technique in our previous work in which, besides applying for the first time the MID technique to examine Ca^{2+} transport, we evaluated the responses to norepinephrine infusion in livers from both healthy and arthritic rats [34]. The MID technique comprises a simultaneous injection of $^{45}\text{Ca}^{2+}$ and indicators into the portal vein and the mathematical analysis of the outflow profiles by means of a space-distributed variable transit time model [35–37]. The technique allows estimating the transfer coefficients for Ca^{2+} influx and efflux from the Ca^{2+} extra- and intracellular spaces and Ca^{2+} pool sizes under conditions in which hemodynamics, anatomy, and hepatocyte polarity are preserved.

The aim of the present study was, thus, to clarify the kinetic mechanisms by which Ni^{2+} affects Ca^{2+} fluxes through various cellular compartments employing the MID technique. It has been suggested that Ni^{2+} acts by depleting intracellular Ca^{2+} stores that are mobilized by hormones [17–19]. Therefore, a comparison between the kinetic changes induced by Ni^{2+} and norepinephrine can provide a better understanding of the Ni^{2+} mode of action. Ca^{2+} transport was evaluated by the MID technique following infusion of exogenous NiCl_2 or norepinephrine into perfused livers. To maximize the interference of Ni^{2+} on Ca^{2+} transport, we have selected the concentration of 1.0 mM NiCl_2 . Despite supraphysiological, this concentration does not impair the liver energy metabolism, as demonstrated by a set of additional experiments in which we examined glycogen catabolism, a biological process that is very sensitive to changes in Ca^{2+} levels and also to cellular energy state [38–40]. To present confirmative evidence of results obtained with the MID experiments, we also performed experiments in cultivated human hepatoma Huh7 cells by evaluating the $[\text{Ca}^{2+}]_c$ using Indo-1 AM.

Materials and methods

Materials

The liver perfusion system and the rapid sampling machine for MID experiments were built in the workshops of the University of Maringá. $^{45}\text{Ca}^{2+}$ (1.7 mCi/mmol), $[^3\text{H}]$ inulin

(0.9 Ci/mmol), $[^3\text{H}]$ water (20 $\mu\text{Ci}/\text{mmol}$), and biodegradable counting scintillant solution (BCS[®]) were purchased from Amersham Life Science (Buckinghamshire, United Kingdom). Inulin and norepinephrine were purchased from Sigma Chemical Company (St. Louis, USA). Indo-1 AM was purchased from Invitrogen (Breda, The Netherlands). Dulbecco's Modified Eagle's Medium (DMEM) was purchased from Gibco, Life Technologies (Carlsbad, USA). All other chemicals were of the best available grade.

Animals and cell culture

Male Holtzman rats weighing 250–300 g and fed ad libitum with a standard laboratory diet (Nuvilab CR-1[®]) were housed in polycarbonate cages in a controlled environment, with a 12 h light–12 h dark cycle starting at 06:00 h, at 20–23 °C. The study was conducted in accordance with the recommendations of the guide for the care and use of laboratory animals and the ethical principles of the National Council for the Control of Animal Experimentation (CONCEA, law n° 11.794, October 8, 2008) and the Ethics Committee on Animal Use (CEUA), State University of Maringá (Resolution n° 004/20160CEP).

Human hepatoma Huh7 cells were originally isolated from a 57-year-old Japanese male with well-differentiated hepatocellular carcinoma [41]. The cells were cultured in culture flasks in DMEM supplemented with 10% fetal bovine serum (FBS), 10% glutamine, 100 U/mL penicillin, and 100 $\mu\text{g}/\text{mL}$ streptomycin. Huh7 cell cultures were maintained at 37 °C and 5% CO_2 .

Liver perfusion experiments

A hemoglobin-free, non-recirculating perfusion was performed according to the technique described by Bracht and Ishii-Iwamoto [42]. For the surgical procedure, the animals were anesthetized by intraperitoneal sodium pentobarbital injection (50 mg/kg body weight). After cannulation of the portal and cava veins, the liver was positioned in a plexiglass chamber. The flow was maintained constant by a peristaltic pump. The perfusion fluid was Krebs/Henseleit bicarbonate buffer (pH 7.4) with serum albumin, saturated with a mixture of oxygen and carbon dioxide (95:5) by means of a membrane oxygenator with simultaneous temperature adjustment at 37 °C. The CaCl_2 concentration in the perfusion fluid was 50 μM . The osmolarity of the perfusion fluid was compensated with NaCl. Only ultra-pure water was used. When required, norepinephrine (1 μM), inulin (1 mM), and NiCl_2 (1 mM) were dissolved in the perfusion fluid. Livers from fed rats were used for all experiments.

The oxygen concentration in the perfusate outflow was continuously monitored by a Teflon-shielded platinum electrode positioned in the plexiglass chamber [43]. The experiments were initiated when steady-state conditions were attained, as judged from the stabilization of oxygen consumption.

MID experiments: general procedures

MID experiments were performed in livers perfused with 50 μM CaCl_2 and 1 mM inulin dissolved in the perfusion fluid. After stabilization of oxygen consumption, 70 μL of a mixture containing $^{45}\text{Ca}^{2+}$ (4.5 μCi), [^3H]inulin (4.5 μCi), and [^3H]water (10 μCi) was injected into the liver [42]. Following injection, the effluent perfusate was initially collected in 0.5–2.0 s fractions over a period of 90 s by means of an automatic fraction collector. The subsequent samples were taken manually in 30–120 s intervals over a period of 1500 s. The samples were added to biodegradable counting scintillant solution (BCS) to measure radioactivity by liquid scintillation, with isotope discrimination for the simultaneous determination of ^3H (as [^3H]inulin and [^3H]water) and total $^{45}\text{Ca}^{2+}$. [^3H]Inulin was counted after elimination of [^3H]water by freeze-drying, and the latter was computed from the difference between total ^3H and [^3H]inulin. An aliquot of the injected mixture was counted to determine the [^3H]inulin to $^{45}\text{Ca}^{2+}$ ratio. The amount of injected $^{45}\text{Ca}^{2+}$ was calculated from this ratio and the recovered [^3H]inulin, which is equal to the injected one [44]. All dilution curves were normalized as [(amount in the effluent sample) \times (s) $^{-1}$ \times (total amount injected) $^{-1}$].

In the presence of 1 mM NiCl_2 , tracers were injected 1.5 min after starting the NiCl_2 infusion. In the presence of

norepinephrine, the tracer injection was done twice during each single experiment: the first 1.5 min after starting the infusion of 1 μM norepinephrine and the second at 30 min after the onset of the hormone infusion.

MID experiments: modeling $^{45}\text{Ca}^{2+}$ behavior in the perfused liver

Suitable equations for the analysis of transport phenomena in the perfused liver can be derived under the assumptions of the space-distributed variable transit time model of Goresky et al. [45] and the kinetic events that underlie the behavior of $^{45}\text{Ca}^{2+}$ in the liver. Based on the innovative study carried in our previous work [34], a four-pool model was formulated. This model is illustrated in Fig. 1, which includes pools, movements, and flow in the vascular space. The four pools are: (1) C_{e1} , the Ca^{2+} concentration in the extracellular space (the portally infused Ca^{2+}); (2) C_{e2} , which corresponds to the Ca^{2+} bound to the cell membrane and adjacencies (e.g., glycocalyx); (3) C_{i1} , which denotes the Ca^{2+} concentration in the first cellular pool (cytosol); and (4) C_{i2} , which corresponds to the Ca^{2+} concentration in the second cellular pool (organelles).

It is assumed that Ca^{2+} in the extracellular space (C_{e1}) rapidly reaches equilibrium with the cell membrane and adjacencies. Thus, the rate parameters for this equilibration tend to infinity (i.e., $\lambda_1 \rightarrow \infty$ and $\lambda_2 \rightarrow \infty$), but their ratio is assumed to be finite (i.e., $\beta = \lambda_1/\lambda_2$). Exchange between the cell membrane pool (C_{e2}) and the first cellular pool (C_{i1}) is assumed to occur with transfer coefficients per unit time and unit space equal to k_1 and k_2 . Similarly, k_3 and k_4 are

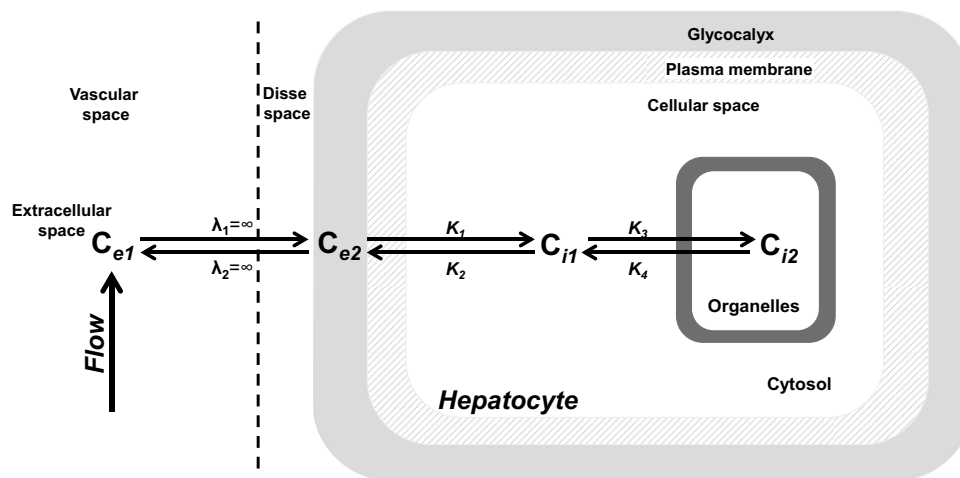


Fig. 1 Schematic representation of the events described by Eq. (1). The scheme is based on the results of the current study and data published by Utsunomiya et al. [34]. Legends: C_{e1} , Ca^{2+} concentration in the extracellular space; C_{e2} , Ca^{2+} concentration in the cell membrane and adjacencies; C_{i1} , Ca^{2+} concentration in the first cellular pool; C_{i2} , Ca^{2+} concentration in the second cellular pool; λ_1 and λ_2 , compos-

ite transfer coefficients for the exchange between the vascular and membrane spaces; k_1 and k_2 , composite transfer coefficients for the exchange between the extracellular space and the first cellular pool; k_3 and k_4 , composite transfer coefficients for the exchange between the first and second cellular pools

the transfer coefficients per unit time and unit space for the exchange between the first and the second cellular pools. For the events in Fig. 1, the liver response to a single injection of $^{45}\text{Ca}^{2+}$ tracer under steady-state circumstances can be expressed by the following equation [34, 44, 46]:

$$Q(t) = Q_{\text{ref}}(t) \times e^{-k_1(t-t_0)} + \int_0^{t-t_0} e^{-k_1\tau} Q_{\text{ref}}(\tau + t_0) \left[e^{\alpha_1(t-t_0-\tau)} \times \sum_{n=1}^{\infty} \frac{[k_1 k_2 (\alpha_1 + k_4) \tau]^n (t - t_0 - \tau)^{n-1}}{(\alpha_1 - \alpha_2)^n n! (n-1)!} \right. \\ \left. + e^{[\alpha_2(t-t_0-\tau)]} \times \sum_{n=1}^{\infty} \frac{[k_1 k_2 (\alpha_2 + k_4) \tau]^n (t - t_0 - \tau)^{n-1}}{(\alpha_2 - \alpha_1)^n n! (n-1)!} \right. \\ \left. + \int_{\tau}^{t-t_0} e^{\alpha_1(\varepsilon-\tau)} \sum_{n=1}^{\infty} \frac{[k_1 k_2 (\alpha_1 + k_4) \tau]^n (\varepsilon - \tau)^{n-1}}{(\alpha_1 - \alpha_2)^n n! (n-1)!} \times e^{[\alpha_2(t-t_0-\varepsilon)]} \times \sum_{n=1}^{\infty} \frac{[k_1 k_2 (\alpha_2 + k_4) \tau]^n (t - t_0 - \varepsilon)^{n-1}}{(\alpha_2 - \alpha_1)^n n! (n-1)!} d\varepsilon \right] d\tau \quad (1)$$

In Eq. (1), $Q(t)$ is the outflow profile of the injected tracer ($^{45}\text{Ca}^{2+}$), where t represents the time after tracer injection, τ specifies the variable transit time in the sinusoids, and t_0 indicates the uniform transit time in the large vessels and catheter. The symbols α_1 and α_2 denote the roots of the quadratic equation: $s^2 + (k_2 + k_3 + k_4)s + k_2 k_4 = 0$. The dimensions of the transfer coefficients are inverse time (s^{-1}), and they are referred to their corresponding distribution space (i.e., $\text{mL s}^{-1} \text{mL distribution space}^{-1}$). For k_1 , this space corresponds to the extracellular space into which $^{45}\text{Ca}^{2+}$ undergoes flow-limited distribution. For k_2 , k_3 , and k_4 , this space corresponds to the intracellular space. $Q_{\text{ref}}(t)$ or $Q_{\text{ref}}(\tau + t_0)$ represents the dilution curve of an appropriate reference for the whole space into which $^{45}\text{Ca}^{2+}$ undergoes flow-limited distribution. This curve can be computed from the outflow profile of [^3H]inulin [$Q_{\text{in}}(t)$], assuming that the appropriate reference differs from [^3H]inulin merely because it distributes in a flow-limited-fashion in an expanded space (Eq. S1.1, S1.2 and S1.3 in Supplementary Material).

MID experiments: estimates of optimized values of transfer coefficients of $^{45}\text{Ca}^{2+}$ transport

Equation (1) was fitted simultaneously to the experimental $^{45}\text{Ca}^{2+}$ outflow profiles together with the previously optimized value of β (Eq. S1.1 in Supplementary material), t_0 (Eq. S1.2, Supplementary material) and provisional estimates of k_1 , k_2 , k_3 , and k_4 . Iterations of the nonlinear least-squares procedures were repeated until the standard deviation of the estimate was minimized. The calculations were done using a specifically designed software program written in the Turbo-Basic language. The integrals in Eq. (1) were calculated by the Romberg's algorithm [47]. Interpolations were done using Stineman's interpolation formula [48].

MID experiments: estimates of Ca^{2+} pool sizes and exchange rates

The Ca^{2+} pool sizes in different compartments C_{e2} , C_{i1} , and C_{i2} shown in Fig. 1 can be calculated from the optimized

Ca^{2+} transfer coefficients and extracellular Ca^{2+} concentration (C_{e1}). These parameters are also required to calculate the rates of influx and efflux of Ca^{2+} across the cell membrane and between the first and second cellular pools ($F_1^{i \leftrightarrow e}$ and $F_2^{i \leftrightarrow e}$, respectively), according to Eq. (S2.1), (S2.2), (S2.3), (S2.4) in Supplementary Material.

Loading of human hepatoma Huh7 cells and determination of $[\text{Ca}^{2+}]_c$ using Indo-1 AM

To conduct Ca^{2+} measurements, the suspension of Huh7 cells was centrifuged at 500g for 3 min, the supernatant was discarded, and the cells were dispersed in Hank's Balanced Salt Solution (HBSS) medium (pH 7.4) containing 1.3 mM CaCl_2 in the absence or presence of 50 μM NiCl_2 . The loading was achieved by incubating the cells for 30 min in a shaking water bath (32 °C) in the presence of 10 μM Indo-1 AM. The cells were then washed twice to remove the residual dye, re-suspended in the same medium, and stored on ice for use. Huh7 cells (2×10^6 cells/mL) were plated in a 96-well microplate. Before measurements, the cells were warmed to 25 °C for 5 min. Excitation wavelength was 340 nm, and fluorescence emitted by the cell was recorded as photon counts per second at 405 (F_{405}) and 520 (F_{520}) nm using the NOVO star microplate reader (BMG Labtech). Calibration and calculation of $[\text{Ca}^{2+}]_c$ were done by the procedure described by Gryniewicz et al. [49]. The maximum (F_{max}) and minimum (F_{min}) fluorescence were obtained by adding ionomycin and ethylene glycol-bis (β -aminoethyl ether)- N,N,N',N' -tetraacetic acid (EGTA) at final concentration of 100 μM and 5 mM, respectively. Variations of the $[\text{Ca}^{2+}]_c$ in Huh7 cells were evaluated before and after the addition of 1 μM norepinephrine. In the present series, a low concentration of NiCl_2 (50 μM) was used to minimize the interference of this metal on Indo-1 AM fluorescence measurements [19, 50].

Liver perfusion analytical assays

To evaluate glycogen catabolism, the livers from fed rats were perfused with a substrate-free medium and samples of the effluent perfusion fluid were collected at specific intervals. The content of glucose, lactate, and pyruvate in the samples was analyzed by standard enzymatic techniques [51]. The oxygen concentration in the perfusate outflow was continuously monitored by a Teflon-shielded platinum electrode. Metabolic rates were calculated from metabolite content in the effluent perfusate and the total flow rates and were referred as the liver wet weights.

Statistical analysis

The data in tables and figures are expressed as mean \pm standard error (SE). The statistical significance of the differences between parameters obtained in the experiments was evaluated with Student's *t* test. The results are discussed in the text using *P* values, where $P < 0.05$ was the criterion used for significance. Statistical analysis was performed using GraphPad software (San Diego, CA, USA).

Results

Typical outflow profiles of $^{45}\text{Ca}^{2+}$ and indicators in the perfused rat liver

Figure 2 shows typical outflow profiles of $^{45}\text{Ca}^{2+}$, [^3H]inulin, and [^3H]water obtained in control livers (Fig. 2a) and livers perfused with Ni^{2+} (Fig. 2b) and norepinephrine infused at 1.5 (Fig. 2c) and 30 min (Fig. 2d). The CaCl_2 concentration in the perfusion fluid was 50 μM in all experiments. This concentration was selected based on our previous work in which Ca^{2+} concentration was assayed at 50, 100, 250 and 500 μM [34]. It was demonstrated that, at concentrations higher than 50 μM , the fraction of tracer ($^{45}\text{Ca}^{2+}$) that enters the cells in a single passage is minimal and its outflow profile does not contain enough information to accurately determine the Ca^{2+} transport kinetic parameters related to intracellular movements of Ca^{2+} [34]. The parameters estimated by the MID under this range of concentration have been demonstrated to be consistent with the current views about the compartmentation of Ca^{2+} and its role as an intracellular messenger [34].

All curves were normalized by dividing the amount of radioactivity that reappeared per second by the total injected radioactivity, considering that there was no loss or irreversible sequestration of the labeled substances in a single passage through the liver [34]. As expected, the [^3H]water outflow profile was delayed relative to that of [^3H]inulin because

water distributes over the entire aqueous space of the liver, whereas [^3H]inulin does not exchange with the cellular space during a single passage. Reproducing the data of our previous work, the $^{45}\text{Ca}^{2+}$ outflow profile had an initial upslope that was slightly delayed (up to 0.5 s) with respect to that of [^3H]inulin until reaching the peak value. This displacement probably occurs due to the additional space occupied by $^{45}\text{Ca}^{2+}$ in a flow-limited distribution from which [^3H]inulin is excluded [34]. Furthermore, the peak time of the $^{45}\text{Ca}^{2+}$ curve was slightly shifted to the right and its downslope decayed more slowly in relation to that of [^3H]inulin, so that both curves crossed soon after the peak time. This finding represents the behavior of the small portion of Ca^{2+} that has access to the aqueous cellular space and returns to the vascular space. These general characteristics of the $^{45}\text{Ca}^{2+}$ curve were reproduced when 1 mM Ni^{2+} or 1 μM norepinephrine were present in the perfusion fluid. Despite similarities of the outflow profiles, only a mathematical analysis of the curves would allow one to assess whether the kinetics of $^{45}\text{Ca}^{2+}$ transport was modified by the different studied conditions. Thus, the estimate of transfer coefficients in the scheme of Fig. 1 was obtained by fitting Eq. (1) and (S1.1 in Supplementary material) to the experimental data. Examples are shown in Fig. 2e–h, which illustrates the results of the calculations from the same representative experiments of a–d, respectively. The closed circles represent the experimental data and the solid lines the calculated curves.

The optimized parameters are given on each graph. There was good agreement between theory and experiment for the set of experiments performed in the absence or presence of Ni^{2+} and norepinephrine (infused at 1.5 and 30 min). The traced line is the new reference $Q_{\text{ref}}(t)$ curve, as given by Eq. (S1.1 in Supplementary material). The curves of the new reference differ from those of [^3H]inulin shown in the previous panels because of an extra, apparent or real, extracellular space into which $^{45}\text{Ca}^{2+}$ undergoes flow-limited distribution, but from which [^3H]inulin is excluded [34]. This $^{45}\text{Ca}^{2+}$ distribution space exceeds that of [^3H]inulin by a relatively small factor, given by $(1 + \beta)$. Table 1 reveals that in the control series, the β parameter was equal to 0.122 ± 0.007 . Ni^{2+} induced a 25% decrease, and norepinephrine did not significantly modify this parameter at 1.5 or 30 min of its infusion in livers compared with the control condition. Equation (1) also allows the resolution of the calculated $^{45}\text{Ca}^{2+}$ outflow profiles into the throughput and exchanged components. The throughput comprises the fraction of the injected $^{45}\text{Ca}^{2+}$ that did not enter the cellular space and crossed only the vascular space, and the exchanged corresponds to the fraction that entered the cells at least once and subsequently returned to the vascular space. These two components are given by the first (throughput) and the second, more complex term (exchanged), in Eq. (1). Figure 2i–m illustrates these separable components of the same set of curves shown in panels

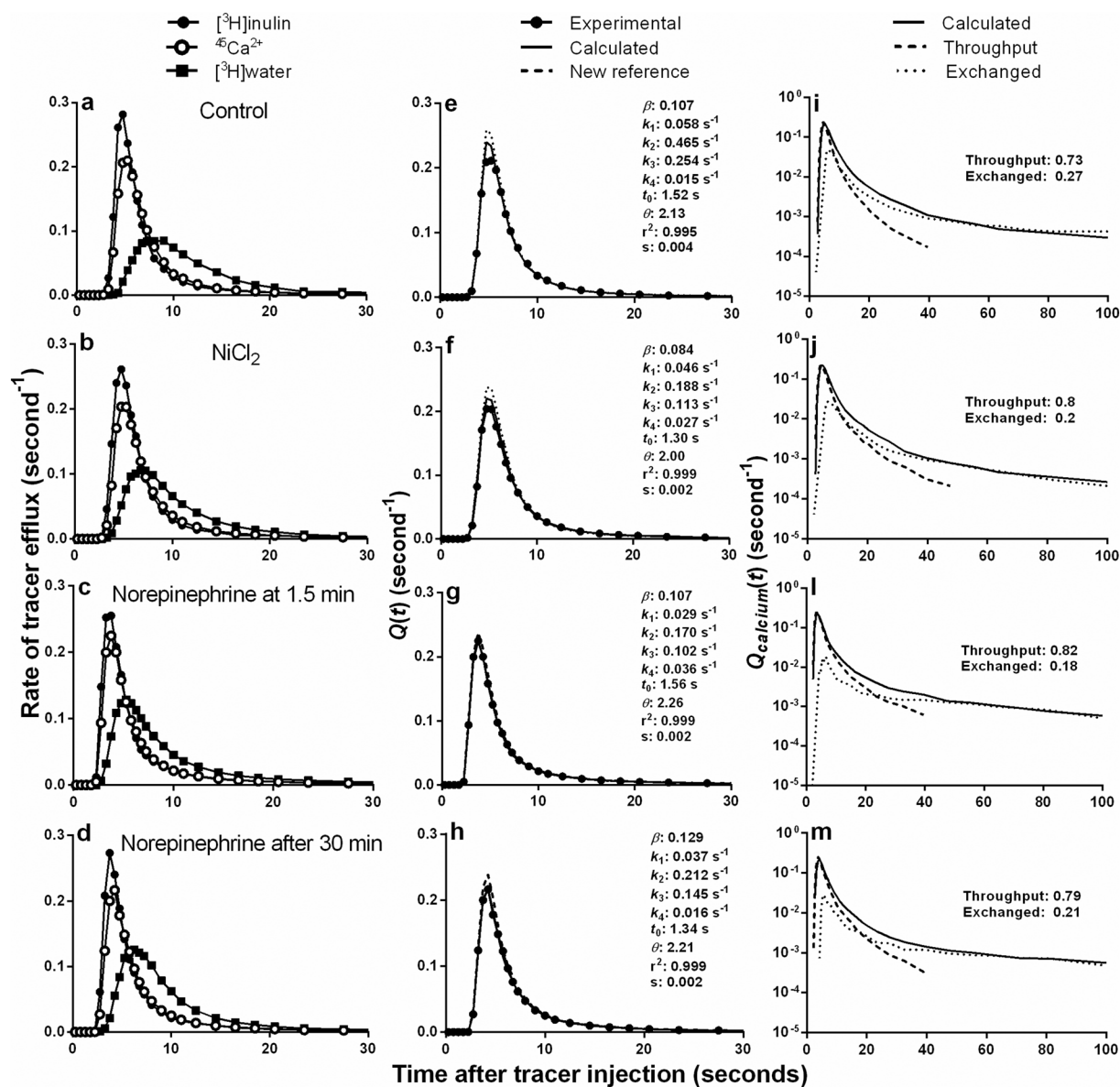


Fig. 2 Typical experimental outflow profiles of $^{45}\text{Ca}^{2+}$ and indicator substances in the absence (Control, **a**) or in the presence of 1 mM NiCl_2 (**b**), and 1 μM norepinephrine at 1.5 min (**c**) or 30 min (**d**) of infusion. Livers were perfused with Krebs–Henseleit bicarbonate buffer (pH 7.4) containing 1 mM inulin and 50 μM CaCl_2 . Trace amounts of ^3H inulin (\bullet – \bullet), $^{45}\text{Ca}^{2+}$ (\circ – \circ), and ^3H water (\blacksquare – \blacksquare) were injected into the portal vein and the outflowing perfusate was fractionated. Fractions of the injected radioactivity of each component appearing in the effluent perfusate per second are represented against the time after injection. **e–h** The theoretical curves of Ca^{2+} and the curve of new reference calculated from the experimental curves of $^{45}\text{Ca}^{2+}$ shown in **a–d** by fitting Eq. (1) and (S1.1 in Supplementary material) to the experimental data. The optimized values

of the various parameters are listed in each graph, together with the standard error of the estimate(s) and the coefficient of determination (r squared). Legends: \bullet , experimental dilution curve of $^{45}\text{Ca}^{2+}$; —, calculated curve employing the optimized parameters; - - -, computed reference curve [$Q_{\text{ref}}(t)$]. **i–m** Resolution of the theoretical $^{45}\text{Ca}^{2+}$ outflow profiles of curves shown in **e** to **h** into their components, throughput and exchanged. The continuous lines represent the calculated curves plotted on a logarithmic scale versus time following injection. The values given on each graph represent the fractions of total injected $^{45}\text{Ca}^{2+}$ that entered (exchanged) or did not enter the cellular space (throughput). The curves of each condition are representative of 4–6 MID experiments

a–d. At 50 μM Ca^{2+} in the perfusion fluid, the $^{45}\text{Ca}^{2+}$ fraction that entered the liver and returned to the perfusate was 23% in the control condition, and neither Ni^{2+} nor norepinephrine significantly modified this parameter (Table 1).

The optimized values obtained from a linear superposition of the ^3H water and ^3H inulin curves, according to Eq. (S1.2 in Supplementary material) and values of the mean transit times of ^3H inulin and ^3H water curves,

Table 1 Effects of 1 mM NiCl₂ or 1 μM norepinephrine on parameters of transport of ⁴⁵Ca²⁺ in rat livers

Parameter	Krebs–Henseleit		Krebs–Henseleit + norepinephrine	
	Control (<i>n</i> = 5)	NiCl ₂ (<i>n</i> = 6)	At 1.5 min (<i>n</i> = 4)	After 30 min (<i>n</i> = 5)
<i>t</i> ₀ (s)	1.601 ± 0.056 ^a	1.407 ± 0.045 ^a (− 12%)	1.476 ± 0.091	1.465 ± 0.042
θ	2.010 ± 0.075	2.062 ± 0.026 ^b	2.190 ± 0.030 ^b (+ 6%)	2.172 ± 0.045
<i>V</i> _v as (flow × <i>t</i> ₀) / (weight × 60)	0.072 ± 0.003	0.066 ± 0.001	0.069 ± 0.004	0.068 ± 0.038
<i>V</i> _e as flow × (<i>t</i> _{in} − <i>t</i> ₀)(ml/g)	0.271 ± 0.011 ^{c,d}	0.307 ± 0.013	0.320 ± 0.004 ^c (+ 18%)	0.314 ± 0.013 ^d (+ 15%)
<i>V</i> _i as flow × (<i>t</i> _{in} − <i>t</i> ₀) × θ (ml/g)	0.546 ± 0.039 ^{e,f,g}	0.632 ± 0.026 ^e (+ 15%)	0.700 ± 0.015 ^f (+ 28%)	0.683 ± 0.033 ^g (+ 25%)
<i>V</i> _i / <i>V</i> _e	2.010 ± 0.075	2.062 ± 0.026 ^h	2.190 ± 0.030 ^h (+ 6%)	2.172 ± 0.045
β	0.122 ± 0.007 ⁱ	0.091 ± 0.006 ^{i,j} (− 25%)	0.094 ± 0.023	0.133 ± 0.009 ^j (+ 46%)
Throughput	0.769 ± 0.020	0.744 ± 0.030	0.774 ± 0.037	0.748 ± 0.054
Exchanged	0.231 ± 0.020	0.256 ± 0.030	0.226 ± 0.037	0.252 ± 0.054

All parameters were obtained from MID experiments performed with 50 μM CaCl₂ in the perfusion fluid, as illustrated in Fig. 2. The parameters were obtained by fitting Eq. (1) and (A.1.1 in Supplementary material) to the experimental outflow profiles. In the NiCl₂ experimental series, the injection of tracers was done 1.5 min after the onset of NiCl₂ infusion. In the norepinephrine experimental series, the injection of tracers was done at 1.5 and 30 min after the onset of the hormone infusion

Values are the mean ± standard errors of 4–6 MID experiments. Identical superscripts indicate significant differences between the values as revealed by Student's *t* test. The 5% level (*P* < 0.05) was adopted as a criterion of significance.

allow the calculation of the vascular (*V*_v), extracellular (*V*_e), and intracellular volumes (*V*_i) of the livers (Table 1). Reproducing the data of our previous work, 1.5 min after norepinephrine infusion, the value of *t*₀ (large vessels transit time) was not different from that of the control, but the *V*_e and *V*_i were increased. These modifications in the liver volumes remained unchanged after 30 min of norepinephrine infusion. In the same way, the intra- to extracellular water space ratio (*V*_i/*V*_e) was not different in livers perfused with norepinephrine irrespective of the infusion time (after 1.5 or 30 min) compared with the control series. The influence of Ni²⁺ on these parameters was quite different from those elicited by norepinephrine. Compared with the control series, Ni²⁺ caused a 12% reduction in *t*₀, with no significant changes in the vascular (*V*_v) and extracellular (*V*_e) volumes, despite a trend toward a higher value of the latter. Similar to the data for norepinephrine, Ni²⁺ caused an increase in the accessible cellular aqueous space (*V*_i) compared with the control condition, with no difference in the parameter *V*_i/*V*_e (Table 1).

The optimized mean values of the transfer coefficients of ⁴⁵Ca²⁺ transport derived from the fitting procedures of Eq. (1) to the experimental data measured in the four experimental conditions are shown in Fig. 3a,b. Also reproducing the data of our previous work [34], at 1.5 min of norepinephrine infusion, the transfer coefficient for Ca²⁺ influx from the extracellular space into the first cellular pool (*k*₁) was not modified, but the transfer coefficient for Ca²⁺ efflux from this pool to the extracellular space (*k*₂) was reduced by 70%. Consequently, the *k*₂/*k*₁ ratio—equal to 18.9 in the control condition—was reduced to 8.1.

The transfer coefficient for Ca²⁺ influx from the first cellular pool into the second compartment (*k*₃) was reduced by 29%. By contrast, the transfer coefficient for Ca²⁺ efflux from this second cellular pool (*k*₄) was strongly stimulated (+ 204%). The combination of these opposite effects led to a strong diminution of the *k*₃/*k*₄ ratio. It was equal to 15.7 in the control condition and reduced to 3.6 in the presence of norepinephrine. The *k*₁/*k*₂ and *k*₃/*k*₄ ratios ultimately reflect the Ca²⁺ concentration gradients between the extra- and intracellular pools, and the modifications caused by norepinephrine were those expected based on knowledge of Ca²⁺-mobilizing hormones [31, 52–54].

After 30 min of norepinephrine infusion, not all the effects were reproduced. The transfer coefficient for Ca²⁺ entry into the second cellular compartment (*k*₃) was not significantly inhibited compared with the control series. The value for Ca²⁺ efflux from this second pool (*k*₄) was similar to that of the control condition and was inhibited at a lower degree than that found at 1.5 min of norepinephrine infusion (−66% relative to the first minutes of norepinephrine infusion). Consequently, the *k*₃/*k*₄ ratio value of 11.1 was significantly higher than that found at 1.5 min of norepinephrine infusion (3.6), approaching the value of the control series (15.7).

On the other hand, the effects on *k*₁ and *k*₂ between the two onset times of norepinephrine infusion were not modified: the transfer coefficient for efflux from the cytosolic pool to the extracellular space (*k*₂) was 52% lower than that of the control condition, and *k*₁ was not altered, although there was a tendency toward a higher value. The *k*₂/*k*₁ ratio value of 8.9 was similar to that found at 1.5 min of the hormone infusion (8.1).

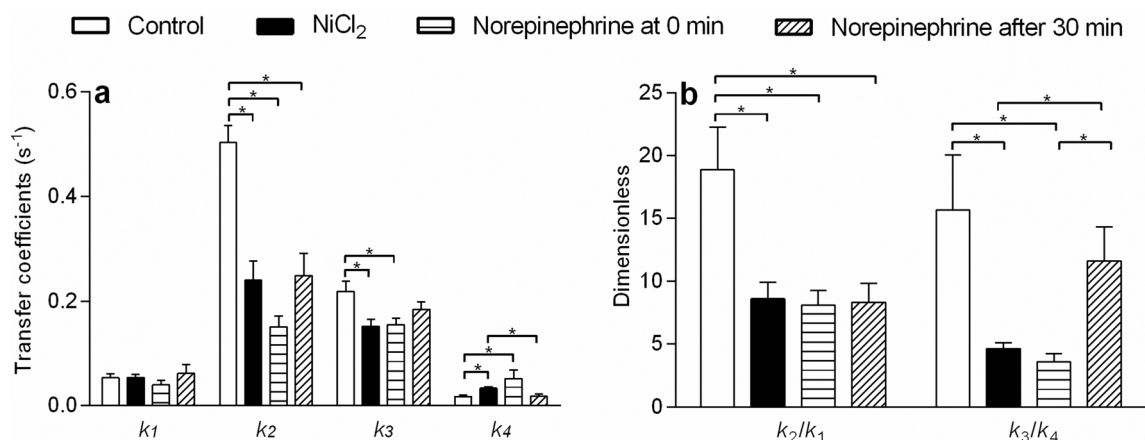


Fig. 3 Transfer coefficients of $^{45}\text{Ca}^{2+}$ transport in the absence (Control) or the presence of 1 mM NiCl_2 or 1 μM norepinephrine (at 1.5 min or 30 min of infusion) (**a**), and the ratios among them (**b**). The mean transfer coefficients were obtained by fitting Eq. (1) and (S1.1 in Supplementary material) to the experimental outflow

The effects of Ni^{2+} in the liver resemble more closely those induced by norepinephrine at 1.5 min of its infusion. Compared with the control series, k_1 was not modified, k_2 was reduced by 52%, k_3 was reduced by 30%, and, in opposition, k_4 was increased by 96%. The combination of these effects led to a diminution of the k_2/k_1 and k_3/k_4 ratios at values similar to those observed in the first minutes of norepinephrine infusion.

The Ca^{2+} pool sizes in different compartments C_{e2} , C_{i1} , and C_{i2} (see Fig. 1) can be calculated by Eq. (S2.1), (S2.3) and (S2.5) in Supplementary material, respectively. C_{e1} corresponds to the portal Ca^{2+} concentration (50 μM) and this value is a component in the Eq. (S2.1) to (S2.5) in Supplementary material. This portal concentration was probably changed during the infusion of Ni^{2+} and norepinephrine, as can be deduced from the modifications in the transfer coefficients for Ca^{2+} transport between the liver compartments. Given that we did not monitor the modifications of the Ca^{2+} portal concentration, under these conditions, the application of Eq. (S2.1) to (S2.5)

profiles of experiments of the kind shown in Fig. 2. Values are the mean \pm standard errors of 4–6 MID experiments. Significance of the differences between the means was derived from Student's *t* test ($P \leq 0.05$) and values differing statistically are indicated by asterisks

(Supplementary Material) is not valid. Thus, Table 2 shows the values obtained only in the control series. At C_{e1} equal to 50 μM , the Ca^{2+} concentration in the first cellular pool (C_{i1}) was 17-fold lower and, thus, the C_{i1}/C_{e1} ratio was smaller than unity; these data corroborate the strong concentration gradient between the vascular and cytosolic spaces (Table 2). The Ca^{2+} concentration in the second cellular pool (C_{i2}) was 13.5-fold higher than that in C_{i1} , resulting in a C_{i2}/C_{i1} ratio equal to 15.6, which is in agreement with the existence of highly concentrated intracellular Ca^{2+} pools (ER and mitochondria). Also reproducing the data of our previous work, the Ca^{2+} exchange rate between the vascular and cytosolic spaces ($F_1^{i \leftrightarrow e}$) was higher than the Ca^{2+} exchange rate between the cytosol and organelles ($F_2^{i \leftrightarrow e}$) (Table 2).

Table 2 The $^{45}\text{Ca}^{2+}$ concentrations, $^{45}\text{Ca}^{2+}$ exchange rates and corresponding ratios in rat livers perfused with 50 μM CaCl_2 (control condition)

Parameter	C_{e2}	C_{i1}	C_{i2}	C_{i1}/C_{e1}	C_{i2}/C_{i1}	$F_1^{i \leftrightarrow e}$	$F_2^{i \leftrightarrow e}$	$F_1^{i \leftrightarrow e} / F_2^{i \leftrightarrow e}$
Control	6.093 ± 0.337	2.960 ± 0.454	39.98 ± 5.79	0.059 ± 0.009	15.66 ± 4.37	0.722 ± 0.102	0.302 ± 0.026	2.414 ± 0.354

The $^{45}\text{Ca}^{2+}$ concentration in the cell membrane and adjacencies (C_{e2}) was calculated according to Eq. (S2.1 in Supplementary material). The $^{45}\text{Ca}^{2+}$ concentrations in the first- (C_{i1}) and second (C_{i2}) cellular pools were calculated according to Eq. (S2.3) and (S2.5) in Supplementary material, respectively. C_{e1} corresponds to the known portally infused Ca^{2+} concentration (50 μM). The rate of $^{45}\text{Ca}^{2+}$ exchange between the extracellular space and the first cellular pool ($F_1^{i \leftrightarrow e}$) and between the first and second cellular pool ($F_2^{i \leftrightarrow e}$) were calculated according to Eq. (S2.2) and (S2.4) in Supplementary material, respectively, using the rate constants derived by fitting Eq. (1) and (S1.1 in Supplementary material) to the outflow profiles. C_{e2} , C_{i1} , and C_{i2} have the dimensions nmol ml^{-1} ; $F_1^{i \leftrightarrow e}$ and $F_2^{i \leftrightarrow e}$ $\text{nmol s}^{-1} \text{ml}^{-1}$. Values are the mean \pm standard errors of five MID experiments

Effects of NiCl₂ on [Ca²⁺]_c in Huh 7 hepatoma cells under norepinephrine stimulation

The modifications in the transfer coefficients k_2 , k_3 , and k_4 found at 1.5 min after starting the norepinephrine infusion agree with the known mode of action of this hormone by increasing the [Ca²⁺]_c, with the mobilization of intracellular stores as the earliest cellular event [31, 53, 54]. The data also corroborate that Ni²⁺ mobilizes Ca²⁺ from intracellular stores and increases the [Ca²⁺]_c [19]. To obtain additional evidence about the Ni²⁺- and norepinephrine-mediated changes in the [Ca²⁺]_c, we evaluated this parameter in cultivated Huh7 hepatoma cells loaded with Indo-1 AM, a cell-permeant intracellular Ca²⁺ indicator. The cells were incubated in the absence or presence of 50 μM NiCl₂ and, after 20 s, 1 μM norepinephrine was added. The [Ca²⁺]_c was measured over 120 s with the fluorophore.

Figure 4a shows the variations in the [Ca²⁺]_c before and after 1 μM norepinephrine addition. The average of the basal [Ca²⁺]_c before the norepinephrine onset in hepatoma cells was 175% higher in the presence of Ni²⁺ compared with the control series. There was a rapid increase in the [Ca²⁺]_c just after norepinephrine addition in the absence (control) or presence of NiCl₂. Subsequently, the levels remained high and reached a steady-state condition above the basal values until the end of the experimental protocol. Visual inspection of the [Ca²⁺]_c curves reveals that, although the similarities between those curves, the kinetic changes induced by

norepinephrine under Ni²⁺ influence was relatively different from that observed in the absence of Ni²⁺, as indicated by Fig. 4b. The ratio between the maximum and basal [Ca²⁺]_c values reached after norepinephrine addition ([Ca²⁺]_{max/bas}) was reduced by 27%, and the ratio between the cytosolic Ca²⁺ concentration at steady-state and basal conditions ([Ca²⁺]_{ste/bas}) was reduced by 32% in the Ni²⁺-cultivated cells compared with control cells.

Effects of NiCl₂ and norepinephrine on liver glycogen catabolism

According to the results presented so far, the Ni²⁺ mode of action shows similarities with the initial action of norepinephrine by affecting the flux of Ca²⁺ transport between extra- and intracellular compartments, resulting in increased [Ca²⁺]_c. Glycogen catabolism is a sensitive indicator of metabolic responses to hormones and other pharmacological agents that trigger an increase in [Ca²⁺]_c [40]. Thus, to investigate the influence of Ni²⁺ on glycogen catabolism, 1 mM NiCl₂ was infused in perfused livers and its effects were compared with those evoked by norepinephrine. This hormone was infused at 1 μM in the absence or presence of 1 mM NiCl₂. The results are shown in Fig. 5. Three parameters were measured: oxygen consumption, glycogenolysis as glucose + ½ (lactate + pyruvate), and glycolysis as lactate + pyruvate.

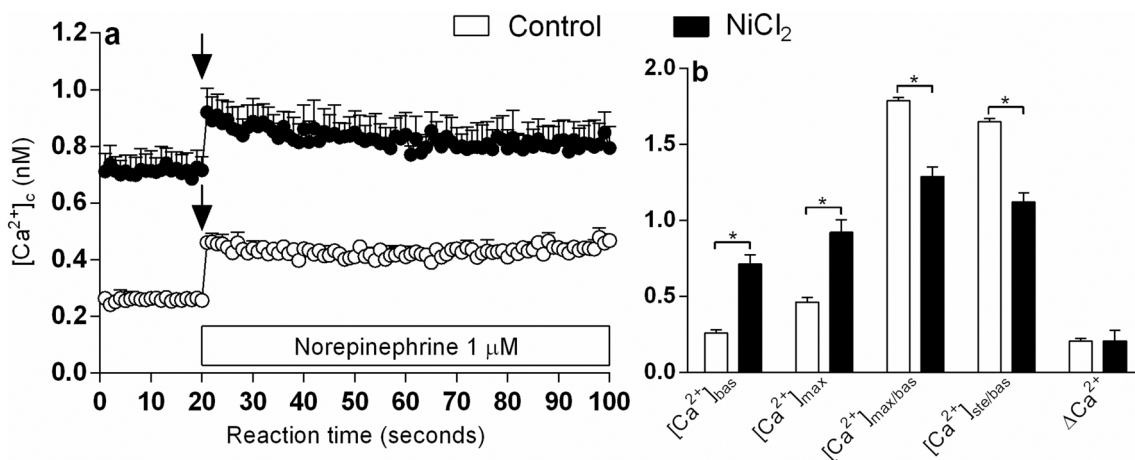


Fig. 4 Effects of norepinephrine on the free cytosolic Ca²⁺ concentration ([Ca²⁺]_c) of cultivated hepatoma Huh 7 cells. Time courses of the changes in the [Ca²⁺]_c in the absence (○—○) and presence (■—■) of 50 μM NiCl₂ (a). The cells were dispersed in Hank's Balanced Salt Solution buffer containing 1.3 mM CaCl₂. Fluorescence due to free Ca²⁺ was recorded before and after the addition of 1 μM norepinephrine (indicated by the arrows). Effects of norepinephrine on the kinetic parameters of the [Ca²⁺]_c in the absence or presence of NiCl₂ (b). The values were obtained from the curves shown in a. Legend: [Ca²⁺]_{basal}: [Ca²⁺]_c before the onset of norepinephrine

(nM); [Ca²⁺]_{max}: maximal [Ca²⁺]_c after the onset of norepinephrine (nM); [Ca²⁺]_{ste}: steady-state [Ca²⁺]_c after the onset of norepinephrine; [Ca²⁺]_{max/bas}: ratio between the maximum and basal [Ca²⁺]_c; [Ca²⁺]_{ste/bas}: ratio between the steady-state and basal [Ca²⁺]_c; ΔCa²⁺: difference of the maximum and basal [Ca²⁺]_c (nM). Each data point and values are the mean of 3–4 experiments with identical protocols. Asterisks indicate significant differences between the values as revealed by Student's *t* test. The 5% level ($P < 0.05$) was adopted as a criterion of significance. Vertical bars represent mean standard errors

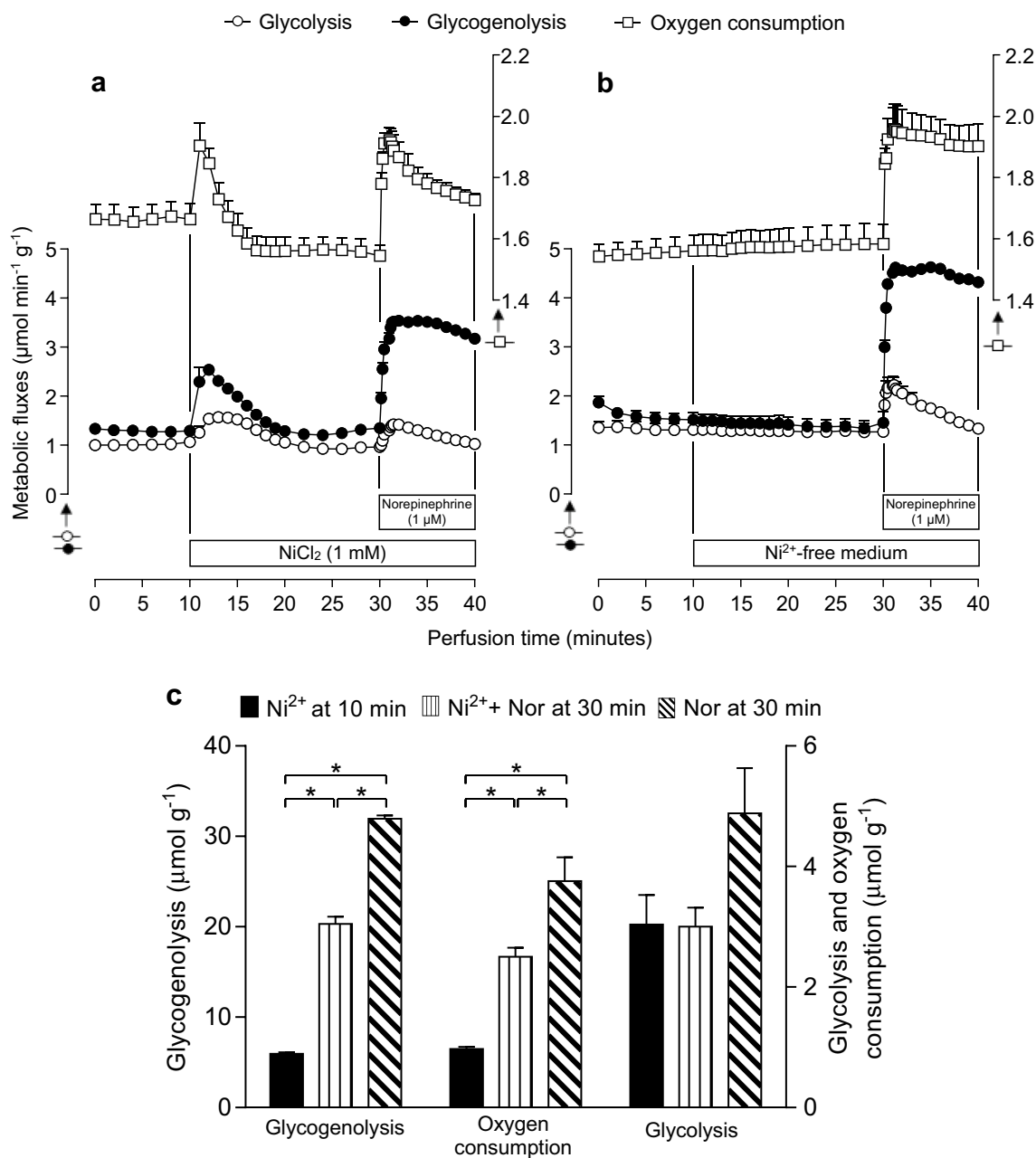


Fig. 5 Influence of Ni²⁺ and norepinephrine in glycolysis, glycogenolysis, and oxygen consumption in perfused livers from fed rats. **a** 1 μM norepinephrine was infused in the presence of Ni²⁺, and **b** in the absence of Ni²⁺ as indicated by horizontal bars. Rates of glycogenolysis and glycolysis were calculated from glucose, lactate, and pyruvate production. Glycogenolysis: glucose + 1/2 (lactate + pyruvate); glycolysis: (lactate + pyruvate). Oxygen was measured polaro-

graphically. **c** Shows the area under the curves of increases in glycolysis, glycogenolysis, and oxygen consumption caused by NiCl₂ (1 mM) and/or norepinephrine (1 μM). Each data point is the mean of four experiments with identical protocols. Asterisks indicate significant differences between the values as revealed by Student's *t* test. The 5% level ($P < 0.05$) was adopted as a criterion of significance. Vertical bars represent mean standard errors

As shown in Fig. 5a, after a pre-perfusion period of 10 min, in which only Krebs–Henseleit buffer was infused, the infusion of 1 mM Ni²⁺ was started; after 20 min, norepinephrine was infused for 10 min together with Ni²⁺. Ni²⁺ infusion induced a rapid increase in all measured parameters, which reached maximum values after 2–4 min from

starting the infusion and, after that, there was a progressive decrease so that a new steady-state condition for all metabolic fluxes was attained after 10 min with the mean values returning to the basal ones (before Ni²⁺ infusion). The exception was for oxygen consumption that reached values below those found before Ni²⁺ infusion. After another

10 min, norepinephrine infusion was started. The introduction of the hormone caused a rapid increment in glycogenolysis, oxygen consumption, and glycolysis. The glycogenolysis rates, besides reaching higher values than those induced by Ni^{2+} at the peak values presented sustained steady-state values during the entire infusion period (10 min). The peak values for oxygen consumption and glycolysis stimulation, which were similar to the maximum peak values induced by the previous Ni^{2+} infusion, gradually recovered toward basal levels. As shown in Fig. 5b, after a 10 min pre-perfusion period in which only Krebs–Henseleit buffer was infused, norepinephrine was infused at the same time interval as that shown in panel a, but without Ni^{2+} in the perfusion fluid.

These experimental series revealed that, in the absence of Ni^{2+} , norepinephrine-induced activation of glycogenolysis and oxygen consumption was higher than those found in the presence of Ni^{2+} . Glycogenolysis and oxygen consumption remained stimulated during the entire period of norepinephrine infusion. On the other hand, glycolysis activation did not reach stable steady-state rates, decreasing gradually toward basal levels. It should be noted that during 1 mM NiCl_2 infusion, there was no evidence of energy impairment in the liver, based on the oxygen consumption that recovered to basal values after following a transient activation. In addition, the oxygen consumption was even activated upon the subsequent norepinephrine infusion.

To facilitate the quantitative comparison between the experimental series, the area under the curve (AUC) for each parameter was calculated; these values are summarized in Fig. 5c. The transitory influence of Ni^{2+} alone led to a 3.4-fold lower AUC for glycogenolysis compared with the one generated by the infusion of norepinephrine (Ni^{2+} + norepinephrine). Glycogenolysis stimulation by the hormone in the absence of Ni^{2+} was higher than the value found in its presence (+57%). There were similar features in the AUC for oxygen consumption stimulation.

Ni^{2+} alone induced a 2.5-fold lower AUC for oxygen consumption stimulation compared with that found during the infusion of norepinephrine (Ni^{2+} + norepinephrine). In the absence of Ni^{2+} , the effect of norepinephrine on oxygen consumption stimulation was 50% higher than that in its presence. The AUC for glycolysis was not significantly different among the groups.

Discussion

In this study, the MID technique was used for the first time to evaluate the effects of Ni^{2+} on liver hemodynamics and Ca^{2+} transport kinetics under steady-state conditions in an intact perfused rat liver. The estimate of the transport transfer coefficients between the extra- and intracellular Ca^{2+} pools and

comparison with changes caused by the Ca^{2+} -mobilizing hormone norepinephrine allowed us to identify the kinetic mechanisms by which Ni^{2+} increases the $[\text{Ca}^{2+}]_c$ and affects a biological response dependent on Ca^{2+} fluxes.

The infusion of 1 mM Ni^{2+} induced changes in the liver hemodynamics, as indicated by a 12% reduction in the t_0 value compared with the control condition. The parameter t_0 represents the sum of the transit times for inflowing and outflowing of large vessels. It is possible that Ni^{2+} induced a constriction at the exit of inflowing large vessels, a phenomenon that in general causes distension in the sinusoids and cells due to the constant flow system of the perfusion fluid in the liver [55]. Indeed, there was an increase in the intravascular volume accessible to water (V_i) ($P < 0.005$) and a tendency toward an increase in the extravascular volume (V_e) in the presence of Ni^{2+} . These Ni^{2+} -evoked hemodynamic effects resembled those caused by norepinephrine at 1.5 min of its infusion, i.e., increases in V_e and V_i . When the experiments were performed after 30 min of norepinephrine infusion, these changes persisted to a similar extent. Consistent with these findings, a previous study demonstrated that norepinephrine and other Ca^{2+} -mobilizing agents, such as vasopressin, phenylephrine, and the ionophore A23187, induce transient vasoconstriction in the liver [56]. Nathanson et al. [29] previously reported a vasoconstrictive effect of Ni^{2+} . The infusion of 25 μM Ni^{2+} increases the portal pressure and decreases the bile flow. Thus, the mechanism by which Ni^{2+} affected liver hemodynamics seems to be similar to that of Ca^{2+} -mobilizing hormones.

Ni^{2+} induced a distinct effect on the Ca^{2+} distribution space in the liver, as indicated by a 25% decrease in the β parameter compared with the control condition. As discussed in our previous work [34], β represents the extra, apparent, or real extracellular space into which $^{45}\text{Ca}^{2+}$ undergoes flow-limited distribution, relative to that occupied by inulin. This space presumably comprises the PM adjacencies including the glycocalyx, where Ca^{2+} can interact with binding sites, such as phospholipids and glycoproteins [57]. By sharing chemical properties with Ca^{2+} , it is possible that Ni^{2+} competes with this ion for the same binding sites, an eventuality that might result in an apparent decrease in the extracellular space of Ca^{2+} represented by β . It should be mentioned that this space was not modified by norepinephrine at the first 1.5 min of its infusion.

The estimate of the transfer coefficients k_1 , k_2 , k_3 and k_4 for Ca^{2+} transport measured at 1.5 min after the infusion of 1 mM Ni^{2+} indicated the modified steps of Ca^{2+} transfer in the perfused liver. The first one was between the first (C_{i1}) and second (C_{i2}) cellular pools. As illustrated by Fig. 1 and based on our previous work [34], C_{i1} corresponds to the cytosolic space and C_{i2} represents the organelles, mainly ER. Ni^{2+} simultaneously induced a diminution in the transfer coefficient for Ca^{2+} entry into the second cellular pool (k_3)

and an increase in the transfer coefficient for Ca^{2+} efflux from this space to the first cellular pool (k_4). The combination of these effects results in an increased net efflux of Ca^{2+} from Ca^{2+} -storing organelles, which can lead to increased $[\text{Ca}^{2+}]_c$. The second step of Ca^{2+} transfer modified by Ni^{2+} was between the first cellular pool (C_{i1}) and the extracellular space (C_{e1}). Ni^{2+} induced a decrease in the transfer coefficient for Ca^{2+} efflux from the cytosolic to extracellular space (k_2). This effect was consistent with a minimization of Ca^{2+} loss due to the increased $[\text{Ca}^{2+}]_c$. There was no significant change in k_1 , indicating that there was not a significant stimulation of the inward transport systems during the first 1.5 min following Ni^{2+} infusion. Our data are in agreement with the work of McNulty and Taylor [19], who reported that Ni^{2+} increases $[\text{Ca}^{2+}]_c$ in hepatocytes due to mobilization of Ca^{2+} from intracellular Ca^{2+} storing organelles with no evidence of an effect of Ni^{2+} on Ca^{2+} inflow from the extracellular into the cytosolic space.

To compare the influence of Ni^{2+} with a Ca^{2+} -mobilizing hormone, we evaluated the kinetic changes of norepinephrine-induced Ca^{2+} transport using the MID technique at 1.5 min and 30 min after the initiation of the hormone infusion. There were significant kinetic differences at 30 min relative to those observed at 1.5 min of the hormone infusion [34]. There was no inhibition in the transfer coefficient k_3 , and the reduction in k_4 was substantially lower at 30 min compared with 1.5 min of norepinephrine infusion. This combination of effects indicates a reduction in the Ca^{2+} exchange rates between the hormone-sensitive cellular pool and the cytosolic space at 30 min compared with the norepinephrine infusion onset at 1.5 min. The concentration gradients between the various pools are reflected by the corresponding ratios of the transfer coefficients for influx and efflux (i.e., k_1/k_2 and k_3/k_4). At 1.5 min of norepinephrine infusion, the increase in the transfer coefficient k_4 with a reduction in k_3 indicate a net efflux of Ca^{2+} from intracellular stores and, thus, a decrease in the concentration gradient between the cytosolic space and the intracellular storage pool due to depletion of these Ca^{2+} stores. The k_3/k_4 ratio, which was 15.7 in the control condition, decreased to 3.6 during the first minutes of norepinephrine infusion. These findings are in agreement with the hypothesis that the mobilization of intracellular stores is the earliest event in the mechanism of action of Ca^{2+} -dependent hormones and that Ca^{2+} entry from the extracellular space into the hepatocytes occurs later on in response to the emptying of the ER Ca^{2+} stores [31, 53, 54]. Indeed, after 30 min of norepinephrine infusion, the lowest absolute increment in k_4 , combined with an unaltered k_3 value, indicates a lower efficiency in mobilizing Ca^{2+} from intracellular stores. The k_3/k_4 ratio—3.6 during the first minutes of norepinephrine infusion—increased to 11.1, a similar value to the control condition. This change is consistent with a restoration of the

second intracellular Ca^{2+} pool. On the other hand, the k_1/k_2 ratio—18.9 in the control condition—decreased to 8.1 and 8.9 at 1.5 and 30 min of norepinephrine infusion, respectively, due to a reduction in k_2 . These data indicate a similar concentration gradient between the extracellular and cytosolic space in these groups.

During the first minutes, Ca^{2+} mobilization from intracellular stores was the main source for the $[\text{Ca}^{2+}]_c$ increment, but under prolonged norepinephrine infusion, Ca^{2+} efflux from intracellular stores (k_4) seems to be prevented, possibly by the dependence of replenishment of this pool on the entry of extracellular Ca^{2+} . These events, along with the reduction of Ca^{2+} efflux from the cytosolic to extracellular space, were the most prominent norepinephrine-induced kinetic changes revealed by the MID technique.

The effects of Ni^{2+} on Ca^{2+} fluxes very closely resembled those caused by norepinephrine at 1.5 min of its infusion. The same transfer coefficients were altered by norepinephrine relative to control ones without significant differences between the absolute values of transfer coefficients measured in the presence of Ni^{2+} and norepinephrine. This finding further supported the conclusion that Ni^{2+} increases the $[\text{Ca}^{2+}]_c$ in intact liver due to mobilization of intracellular Ca^{2+} stores along with reduction of Ca^{2+} efflux from the cytosolic space.

The Huh7 cell line data corroborated the Ni^{2+} -induced $[\text{Ca}^{2+}]_c$ increase. The basal Ca^{2+} concentration value was higher in the presence of Ni^{2+} and, in relative terms, the $[\text{Ca}^{2+}]_c$ rise induced by the subsequent norepinephrine addition was lower in these cells, as indicated by reduction in the $[\text{Ca}^{2+}]_{\text{max/bas}}$ ratio. These results are in line with those previously reported by McNulty and Taylor [19], who showed that, in cultivated primary hepatocytes, Ni^{2+} partially compromises the action of Ca^{2+} -mobilizing hormones, a finding that Karjalainen and Bygrave [28] also found in perfused livers.

We have demonstrated that the modifications of cellular Ca^{2+} fluxes by Ni^{2+} are translated into a modification in the hepatic glycogen catabolism, also perturbing the norepinephrine regulatory action on this process. Continuous Ni^{2+} infusion in the perfused liver led to a rapid but transient glycogenolysis and glycolysis activation, an effect that differed from what occurred in the presence of norepinephrine, which induced a steady-state stimulation of both processes during the entire hormone infusion. The transient glycogenolysis stimulation is in accordance with the transient Ni^{2+} -induced $[\text{Ca}^{2+}]_c$ increase in different isolated cells [17–19]. Glycogenolysis stimulation possibly contributes for the Ni^{2+} -induced hyperglycemia reported in some organisms, such as goldfish [58] and rats [3, 59].

It is known that norepinephrine stimulates liver glycogenolysis by both cyclic adenosine monophosphate (cAMP)-dependent (β -adrenergic receptors) and Ca^{2+} -dependent (α -adrenergic receptor) mechanisms. Changes in the $[\text{Ca}^{2+}]_c$

through the IP_3 pathway play a fundamental role in regulating glucose homeostasis by negatively and positively regulating the activities of glycogen synthase and phosphorylase, respectively [60, 61]. The first event in the norepinephrine-induced increase in the $[Ca^{2+}]_c$ is the IP_3 -induced release of Ca^{2+} from internal stores, mainly ER [31, 52–54]. After depletion of these stores, the $[Ca^{2+}]_c$ increase depends on Ca^{2+} inflow from the extracellular space through store-operated calcium channels (SOCs) activation that, in turn, activates sarco/ER Ca^{2+} -ATPase (SERCA) to restore ER Ca^{2+} stores [31, 62, 63]. Our kinetic data of the Ca^{2+} transfer estimated in the presence of norepinephrine were consistent with these molecular mechanisms as discussed above.

Thus, it seems likely that Ni^{2+} activates only the early mechanisms by which norepinephrine activates glycogenolysis, but not those involved in the subsequent sustained stimulation. Moreover, consistent with the interference of Ni^{2+} on norepinephrine-induced $[Ca^{2+}]_c$ increase in Huh7 cells, the glycogenolysis stimulation induced by the subsequent norepinephrine infusion was partially reduced in the presence of Ni^{2+} .

The transfer coefficients estimated by the MID technique are composite parameters: they are functions of the Ca^{2+} concentration in the pertinent compartment, the binding degree of Ca^{2+} to various sites, and the kinetic constants of the carrier systems responsible for the transfer across membranes (basically K_M and V_{max}). The comparison between the Ni^{2+} - and norepinephrine-induced kinetic changes, their effects on perfused intact liver and Huh7 cells, and knowledge of the carrier systems implicated in the regulation of the cellular Ca^{2+} concentrations, allowed us to suggest at least two mechanisms by which Ni^{2+} affected hepatic Ca^{2+} fluxes: (1) stimulation of Ca^{2+} release from intracellular stores by stimulating a transport system responsible for the release of Ca^{2+} from ER, together with inhibition of Ca^{2+} uptake in a reverse flow through an energy-dependent transporter; and (2) inhibition of Ca^{2+} efflux from the cytosolic to the extracellular space, also an energy-dependent transport event.

An increase in the Ni^{2+} -induced Ca^{2+} release from intracellular stores seems to be receptor mediated and possibly occurs through activation of CaSR, a member of the G-protein-coupled receptor superfamily [20, 21]. This receptor, first characterized in the parathyroid gland and kidney, is activated by several di- and trivalent cations, including the extracellular Ca^{2+} , barium (Ba^{2+}), Cd^{2+} , cobalt (Co^{2+}), iron (Fe^{2+}), Gd^{3+} , lead (Pb^{2+}), and Ni^{2+} [18, 20, 22]. In human-cultured airway epithelial cells, Cortijo et al. [18] demonstrated that the Ni^{2+} -induced $[Ca^{2+}]_c$ transient increase is suppressed when the ER Ca^{2+} stores are depleted using thapsigargin or ryanodine but not by removing Ca^{2+} from the medium. The Ni^{2+} effect is reduced by inhibition of PLC or IP_3 release, indicating activation of the G_q -signaling.

Involvement of the CaSR in these effects has been evidenced by messenger RNA (mRNA) and protein expression and abolishment of the Ca^{2+} response to Ni^{2+} using a CaSR antagonist [18]. Canaff et al. [64] demonstrated that CaSR is expressed in the liver and that its known agonists Gd^{3+} and spermine increase the $[Ca^{2+}]_c$ in isolated rat hepatocytes loaded with Fura-2 AM. Although the direct effect of Ni^{2+} on hepatic CaSR remains to be confirmed, similar actions on the Ca^{2+} fluxes and Ca^{2+} -sensitive biological responses consist strong evidence that the increased Ca^{2+} release from intracellular stores may be induced by activation of the hepatic CaSR.

Our MID experiments revealed that the Ni^{2+} -induced increase in Ca^{2+} release from the intracellular stores was the consequence of an augmented Ca^{2+} efflux (k_4) as well as the inhibition of Ca^{2+} inflow (k_3), as it was also observed when norepinephrine was infused for 1.5 min. SERCA is the main transporter that actively translocates Ca^{2+} from the cytosol to internal ER stores [63, 65]. A reduction in Ca^{2+} inflow to intracellular stores (k_3) by Ni^{2+} could be secondary to its action on CaSR signaling, or it could be due to a direct action on SERCA. The latter assumption is supported by the observation that divalent metal cations, such as Cd^{2+} , Cu^{2+} and Zn^{2+} , inhibit Ca^{2+} uptake and induce a prompt Ca^{2+} efflux from preloaded hepatic microsomal vesicles [66].

The second mechanism by which Ni^{2+} increases the $[Ca^{2+}]_c$ was revealed by a decrease in the transfer coefficient of Ca^{2+} efflux from the cytosolic to vascular space (k_2). The major transporter involved in this process is the PM Ca^{2+} -ATPase (PMCA), which is known to play a major role in the long-term control of intracellular free Ca^{2+} levels in eukaryotic cells [67]. This transporter is negatively modulated by different Ca^{2+} -mobilizing hormones, including vasopressin, angiotensin, and $\alpha 1$ -adrenergic hormones [68]. The finding that norepinephrine also reduced the k_2 transfer coefficient supports the hypothesis that reduced PMCA activity may have contributed to the reduced k_2 transfer coefficient values, resulting in the diminished Ca^{2+} transport out of the cell through the PM and, thus, contributing to the $[Ca^{2+}]_c$ increase. A direct interference of Ni^{2+} on PMCA is a possibility to be considered based on a report that vanadate and various metals, such as lanthanum (La^{3+}) and Pb^{2+} , inhibit PMCA activity [69].

A question that remains to be clarified is the inability of Ni^{2+} to sustain glycogenolysis stimulation, a phenomenon possibly related to the transient nature of Ni^{2+} -induced $[Ca^{2+}]_c$ increase reported in different cells [17–19]. It is known that after the initial ER Ca^{2+} store depletion by Ca^{2+} -mobilizing hormones and by receptor-independent mechanisms, such as what occurs with the use of thapsigargin [65], the increase in $[Ca^{2+}]_c$ depends on refilling ER Ca^{2+} stores through SOCs. This mechanism was apparently not activated after Ni^{2+} -induced mobilization of intracellular

Ca²⁺ stores. Nevertheless, it seems that Ni²⁺-mobilized intracellular stores were refilled, as even in the presence of Ni²⁺, norepinephrine further increased the [Ca²⁺]_c in Huh7 cells, with only a small reduction in its maximal extent. Furthermore, the norepinephrine infusion in the perfused liver induced a sustained glycogenolysis activation even after the Ni²⁺ infusion, which alone had evoked a transient stimulation. Cortijo et al. [18] reported similar observations in lung cells. The transient effect of Ni²⁺ on [Ca²⁺]_c is repeatable, indicating restoration of the intracellular Ca²⁺ stores. The mechanism for ER refilling would involve other Ca²⁺ transporters in the membrane systems of hepatocytes, including non-store-operated PM Ca²⁺-permeable channels [31].

Another Ni²⁺ effect that deserves a comment is the partial reduction in the effects of norepinephrine in Huh7 cells and perfused livers. The Ni²⁺-mediated interference on responses to Ca²⁺ agonists, such as glucagon and vasopressin, has also been reported by other authors [19, 28]. This effect may be related to the report of Jiang et al. [70], which showed that, in human 7721 hepatoma cells, Ni²⁺ blocks the increase in [Ca²⁺]_c due to extracellular CaCl₂ addition in thapsigargin-pretreated cells. This effect, which suggests that Ni²⁺ may exert an inhibitory effect on SOCs, is supported by the similarities of Ni²⁺ actions with those induced by 2-amino-ethyl-diphenyl borate (2-APB), a compound that has been demonstrated to inhibit SOCs by binding to its channel protein or an associated regulatory protein [71]. In isolated liver cells, 2-APB also induces Ca²⁺ release from intracellular stores and inhibits thapsigargin- and vasopressin-stimulated Ca²⁺ inflow, with no effect on Ca²⁺ release from intracellular stores induced by these agonists [71]. Ni²⁺ seems to have a distinct mode of action in contractile tissues, such as cardiac and vascular tissues, possibly due to the involvement of different Ca²⁺ channels in these tissues such as the voltage-regulated Ca²⁺ channels [72–74]. Wani et al. [74], for example, have demonstrated that nickel increases phenylephrine-induced contraction in isolated segments of the rat aorta, through an increase in voltage-regulated T-type Ca²⁺ influx, with no role for L-type calcium channels and SOCs.

It is worth mentioning that the suggestion of involvement of the molecular identities CaSR, SERCA, PMCA, SOCs, and non-store-operated PM Ca²⁺-permeable channels in the mechanisms of Ni²⁺ actions in intact livers, though based on a good correlation between several observations from the present study and literature data [20, 21, 31, 62, 63, 67] certainly needs to be confirmed.

A question that deserves a final comment is the physiological relevance of the effects exerted by 1.0 mM Ni²⁺ in the isolated perfused rat liver. In a population without significant occupational exposure, there was an estimated average Ni²⁺ intake of nearly 150 µg day⁻¹ [75, 76]. In human liver biopsy samples, Varga et al. [77] found uneven

Ni²⁺ concentrations that ranged from 0.7 to 15 µg g⁻¹ (dry weight) and several samples with extremely high Ni²⁺ concentrations (36–693 µg g⁻¹). The authors found a correlation with hepatic steatosis and Ni²⁺ concentrations exceeding 15 µg g⁻¹ (dry weight). In the aqueous space of liver cells, 15 µg g⁻¹ (dry weight) corresponds to an intracellular Ni²⁺ concentration of 0.05 mM; the reported range of high concentrations of 36–693 µg g⁻¹ corresponding to 4–46 mM. Thus, it is reasonable to assume that even exposure to serum doses below 1.0 mM for prolonged periods can lead to hepatic Ni²⁺ accumulation in a concentration range that might perturb Ca²⁺ homeostasis and the liver functions, and also alter other metabolic functions mediated by Ca²⁺ in different organs.

Conclusion

We have presented evidence using the MID technique that the kinetic parameters of Ca²⁺ transport modified by Ni²⁺ in intact liver are very similar to those modified by norepinephrine in its first minute of action, but the membrane receptors or Ca²⁺ transporters affected by Ni²⁺ seem to be distinct from those known to be modulated by norepinephrine.

Supplementary Information The online version contains supplementary material available at <https://doi.org/10.1007/s00775-021-01883-7>.

Author contributions KSU: Investigation, validation, formal analysis, writing—original draft. LJdS: Investigation, validation. JI: Investigation, validation. RPC: Visualization, writing—review and editing. EHG: Visualization. JC: Writing—review and editing. AB: Methodology, software. RPJOE: Supervision, writing—review and editing. ELI-I: Supervision, project administration, funding acquisition, writing—original draft, review and editing.

Funding This work was supported by grants from the Conselho Nacional de Desenvolvimento Científico e Tecnológico (CNPq—308980/2017–4) and Coordenação de Aperfeiçoamento de Pessoal do Ensino Superior (CAPES/NUFFIC n°14/10). Karina Sayuri Utsunomiya holds fellowship from the Conselho Nacional de Desenvolvimento Científico e Tecnológico.

Availability of data and material All data generated or analyzed during this study are included in this published article and its supplementary information files.

Code availability Not applicable.

Declarations

Conflict of interest The authors declare that they have no conflict of interest.

Ethics approval All experiments were conducted in strict adherence with the guidelines of the National Council for the Control of Animal Experimentation CONCEA (law no. 11.794 October 8, 2008) and The

Ethics Committee on Animal Use (CEUA), of the State University of Maringá (Resolution n° 004/2016OCEP), which follows the internationally accepted recommendations for the care and use of animals.

References


- Kumar S, Trivedi AV (2016) A review on role of nickel in the biological system. *Int J Curr Microbiol Appl Sci* 5:719–727. <https://doi.org/10.20546/ijcmas.2016.503.084>
- Zambelli B, Ciurli S (2013) Nickel and human health. *Met Ions Life Sci* 13:321–357. https://doi.org/10.1007/978-94-007-7500-8_10
- Tikare SN, Das GA, Dhundasi SA, Das KK (2008) Effect of antioxidants l-ascorbic acid and alpha-tocopherol supplementation in nickel exposed hyperglycemic rats. *J Basic Clin Physiol Pharmacol* 19:89–102. <https://doi.org/10.1515/JBCPP.2008.19.2.89>
- Zelicoff JT, Thomas P (1998) Immunotoxicology of environmental and occupational metals. CRC Press, Boca Raton
- Palermo FF, Risso WE, Simonato JD, Martinez CBR (2015) Bioaccumulation of nickel and its biochemical and genotoxic effects on juveniles of the neotropical fish *Prochilodus lineatus*. *Ecotoxicol Environ Saf* 116:19–28. <https://doi.org/10.1016/j.ecoenv.2015.02.032>
- Sunderman FW, Aitio A, Morgan LG, Norseth T (1986) Biological monitoring of nickel. *Toxicol Ind Health* 2:17–78. <https://doi.org/10.1177/074823378600200102>
- Vijver MG, Van Gestel CAM, Lanno RP et al (2004) Internal metal sequestration and its ecotoxicological relevance: a review. *Environ Sci Technol* 38:4705–4712. <https://doi.org/10.1021/es040354g>
- Adjroud O (2013) The toxic effects of nickel chloride on liver, erythropoiesis, and development in Wistar albino preimplanted rats can be reversed with selenium pretreatment. *Environ Toxicol* 28:290–298. <https://doi.org/10.1002/tox.20719>
- Buxton S, Garman E, Heim KE et al (2019) Concise review of nickel human health toxicology and ecotoxicology. *Inorganics* 7:89. <https://doi.org/10.3390/inorganics7070089>
- Haber LT, Erdreich L, Diamond GL et al (2000) Hazard identification and dose response of inhaled nickel-soluble salts. *Regul Toxicol Pharmacol* 31:210–230. <https://doi.org/10.1006/rtp.2000.1377>
- Bai YN, Yang AM, Pu HQ et al (2014) Nickel-exposed workers in China: a cohort study. *Biomed Environ Sci* 27:208–211. <https://doi.org/10.3967/bes.2014.042>
- Coogan TP, Latta DM, Snow ET, Costa M (1989) Toxicity and carcinogenicity of nickel compounds. *Crit Rev Toxicol* 19:341–384. <https://doi.org/10.3109/10408448909029327>
- Kasprzak KS, Sunderman FW, Salnikow K (2003) Nickel carcinogenesis. *Mutat Res Fundam Mol Mech Mutagen* 533:67–97. <https://doi.org/10.1016/j.mrfmmm.2003.08.021>
- Novelli ELB, Rodrigues NL, Sforzin JM, Ribas BO (1997) Toxic effects of nickel exposure on heart and liver of rats. *Toxic Subst Mech* 16:251–258. <https://doi.org/10.1080/10769189729612>
- Nieboer E (1975) The lanthanide ions as structural probes in biological and model systems. *Struct Bond*. <https://doi.org/10.1007/bfb0116554>
- Evans CH (1990) Biochemistry of the Lanthanides. Plenum Press, New York
- Adebanjo OA, Igietseme J, Huang CLH, Zaidi M (1998) The effect of extracellularly applied divalent cations on cytosolic Ca^{2+} in murine Leydig cells: evidence for a Ca^{2+} -sensing receptor. *J Physiol* 513:399–410. <https://doi.org/10.1111/j.1469-7793.1998.399bb.x>
- Cortijo J, Milara J, Mata M et al (2010) Nickel induces intracellular calcium mobilization and pathophysiological responses in human cultured airway epithelial cells. *Chem Biol Interact* 183:25–33. <https://doi.org/10.1016/j.cbi.2009.09.011>
- McNulty TJ, Taylor CW (1999) Extracellular heavy-metal ions stimulate Ca^{2+} mobilization in hepatocytes. *Biochem J* 339:555–561. <https://doi.org/10.1042/0264-6021:3390555>
- Handlogten ME, Shiraishi N, Awata H et al (2000) Extracellular Ca^{2+} -sensing receptor is a promiscuous divalent cation sensor that responds to lead. *Am J Physiol Ren Physiol* 279:1083–1091. <https://doi.org/10.1152/ajprenal.2000.279.6.f1083>
- Ward DT (2004) Calcium receptor-mediated intracellular signaling. *Cell Calcium* 35:217–228. <https://doi.org/10.1016/j.ceca.2003.10.017>
- Brown EM, MacLeod RJ (2001) Extracellular calcium sensing and signalling. *Physiol Rev* 81:239–297. <https://doi.org/10.1152/physrev.2001.81.1.239>
- Arias IM, Boyer JL, Fausto N et al (1994) The liver: biology and pathobiology. Raven Press, New York
- Blazka ME, Shaikh ZA (1992) Cadmium and mercury accumulation in rat hepatocytes: interactions with other metal ions. *Toxicol Appl Pharmacol* 113:118–125. [https://doi.org/10.1016/0041-008X\(92\)90015-K](https://doi.org/10.1016/0041-008X(92)90015-K)
- Funakoshi T, Inoue T, Shimada H, Kojima S (1997) The mechanisms of nickel uptake by rat primary hepatocyte cultures: role of calcium channels. *Toxicology* 124:21–26. [https://doi.org/10.1016/S0300-483X\(97\)00131-5](https://doi.org/10.1016/S0300-483X(97)00131-5)
- Boyer J (2002). In: Schiff ER, Sorrell MF, Maddrey WC (eds) Schiff's diseases of the liver. Williams & Wilkins, Philadelphia
- Dixon CJ, White PJ, Hall JF et al (2005) Regulation of human hepatocytes by P2Y receptors: control of glycogen phosphorylase, Ca^{2+} , and mitogen-activated protein kinases. *J Pharmacol Exp Ther* 313:1305–1313. <https://doi.org/10.1124/jpet.104.082743>
- Karjalainen A, Bygrave FL (1995) Nickel: an agent for investigating the relation between hormone-induced Ca^{2+} influx and bile flow in the perfused rat liver. *Cell Calcium* 18:214–222. [https://doi.org/10.1016/0143-4160\(95\)90066-7](https://doi.org/10.1016/0143-4160(95)90066-7)
- Nathanson MH, Gautam A, Bruck R et al (1992) Effects of Ca^{2+} agonists on cytosolic Ca^{2+} in isolated hepatocytes and on bile secretion in the isolated perfused rat liver. *Hepatology* 15:107–116. <https://doi.org/10.1002/hep.1840150119>
- Hughes BP, Barritt GJ (1989) Inhibition of the liver cell receptor-activated Ca^{2+} inflow system by metal ion inhibitors of voltage-operated Ca^{2+} channels but not by other inhibitors of Ca^{2+} inflow. *BBA - Mol Cell Res* 1013:197–205. [https://doi.org/10.1016/0167-4889\(89\)90135-3](https://doi.org/10.1016/0167-4889(89)90135-3)
- Barritt GJ, Chen J, Rychkov GY (2008) Ca^{2+} -permeable channels in the hepatocyte plasma membrane and their roles in hepatocyte physiology. *Biochim Biophys Acta Mol Cell Res* 1783:651–672. <https://doi.org/10.1016/j.bbamcr.2008.01.016>
- Berridge MJ (2002) The endoplasmic reticulum: a multifunctional signaling organelle. *Cell Calcium* 32:235–249. <https://doi.org/10.1016/S0143416002001823>
- Zegers MMP, Hoekstra D (1998) Mechanisms and functional features of polarized membrane traffic in epithelial and hepatic cells. *Biochem J* 336:257–269. <https://doi.org/10.1042/bj3360257>
- Utsunomiya KS, Scaliante LG, Bracht A, Ishii-Iwamoto EL (2013) Transport and distribution of $^{45}Ca^{2+}$ in the perfused rat liver and the influence of adjuvant-induced arthritis. *Biochim Biophys Acta Mol Basis Dis* 1832:249–262. <https://doi.org/10.1016/j.bbadis.2012.10.008>
- Ferraresi-Filho O, Ishii-Iwamoto EL, Bracht A (1997) Transport, metabolism and distribution space of octanoate in the perfused rat liver. *Cell Biochem Funct* 15:69–80. <https://doi.org/10.1002>

- (SICI)1099-0844(19970601)15:2%3c69::AID-CBF721%3e3.0.CO;2-H
36. Goresky CA, Bach GC, Nadeau BE (1973) On the uptake of materials by the intact liver. The transport and net removal of galactose. *J Clin Invest* 52:991–1009. <https://doi.org/10.1172/JCI107300>
 37. Schwab AJ, Bracht A, Scholz R (1979) Transport of d-Lactate in Perfused Rat Liver. *Eur J Biochem* 102:537–548. <https://doi.org/10.1111/j.1432-1033.1979.tb04270.x>
 38. Fedatto-Júnior Z, Ishii-Iwamoto EL, Caparroz-Assef SM et al (2002) Glycogen levels and glycogen catabolism in livers from arthritic rats. *Mol Cell Biochem* 229:1–7. <https://doi.org/10.1023/A:1017913124084>
 39. do Nascimento GS, Constantin RP, Gilglioni EH et al (2018) The acute effects of citrus flavanones on the metabolism of glycogen and monosaccharides in the isolated perfused rat liver. *Toxicol Lett* 291:158–172. <https://doi.org/10.1016/j.toxlet.2018.04.001>
 40. Yamamoto NS, Ishii-Iwamoto EL, Bracht A (1992) Activation of glycogenolysis by methotrexate. Influence of calcium and inhibitors of hormone action. *Biochem Pharmacol* 44:761–767. [https://doi.org/10.1016/0006-2952\(92\)90414-e](https://doi.org/10.1016/0006-2952(92)90414-e)
 41. Nakabayashi H, Miyano K, Sato J et al (1982) Growth of human hepatoma cell lines with differentiated functions in chemically defined medium. *Cancer Res* 42:3858–3863
 42. Bracht A, Ishii-Iwamoto EL (2003) Métodos de Laboratório em Bioquímica. Manole, São Paulo
 43. Clark LC (1956) Monitoring and control of blood O₂ tension. *Trans Am Soc Artif Intern Organs* 2:41–49
 44. Bracht A, Schwab AJ, Scholz R (1980) Untersuchung von flüßgeschwindigkeiten in der isolierten perfundierten rattenleber durch pulsmarkierung mit radioaktiven substraten und mathematischer analyse der auswaschkinetiken. *Hoppe Seylers Z Physiol Chem* 361:357–378. <https://doi.org/10.1515/bchm2.1980.361.1.357>
 45. Goresky CA, Ziegler WH, Bach GG, Wangel B (1970) Capillary exchange modeling. *Circ Res* 27:739–764. <https://doi.org/10.1161/01.res.27.5.739>
 46. Rose CP, Goresky CA, Bach GG (1977) The capillary and sarcolemmal barriers in the heart. An exploration of labeled water permeability. *Circ Res* 41:515–533. <https://doi.org/10.1161/01.RES.41.4.515>
 47. Björck A, Dahlquist G (1972) Numerische methoden. Oldenbourg Verlag, Munich
 48. Wagon S (1999) Mathematica in action. Springer Science & Business Media, St. Paul
 49. Grynkiewicz G, Poenie M, Tsien RY (1985) A new generation of Ca²⁺ indicators with greatly improved fluorescence properties. *J Biol Chem* 260:3440–3450. [https://doi.org/10.1016/s0021-9258\(19\)83641-4](https://doi.org/10.1016/s0021-9258(19)83641-4)
 50. Terracciano CMN, MacLeod KT (1996) Reloading of Ca²⁺-depleted sarcoplasmic reticulum during rest in guinea pig ventricular myocytes. *Am J Physiol Hear Circ Physiol* 271:H1814–H1822. <https://doi.org/10.1152/ajpheart.1996.271.5.h1814>
 51. Bergmeyer HU (1974) Methods of enzymatic analysis. Academic Press, New York
 52. Hansen CA, Yang L, Williamson JR (1991) Mechanisms of receptor-mediated Ca²⁺ signaling in rat hepatocytes. *J Biol Chem* 266:18573–18579. [https://doi.org/10.1016/s0021-9258\(18\)55101-2](https://doi.org/10.1016/s0021-9258(18)55101-2)
 53. Putney JW Jr, Aub DL, Taylor CW, Merritt JE (1986) Formation and biological action of inositol 1,4,5-trisphosphate. *Fed Proc* 45:2634–2638
 54. Reinhart PH, Taylor WM, Bygrave FL (1984) The action of α -adrenergic agonists on plasma-membrane calcium fluxes in perfused rat liver. *Biochem J* 220:43–50. <https://doi.org/10.1042/bj2200043>
 55. Polato-Schmeisch A, Suzuki-Kemmelmeier F, Bracht A (2005) The Ca²⁺ mediated metabolic hemodynamic effects of vasopressin in the liver. *Trends Cell Mol Biol* 1:35–50
 56. Withrington PG, Richardson PDI (1990). In: Zakim D, Boyer TD (eds) *Hepatology*. W.B. Saunders, Philadelphia
 57. Shlatz L, Marinetti GV (1972) Calcium binding to the rat liver plasma membrane. *Biochim Biophys Acta* 290:70–83. [https://doi.org/10.1016/0005-2736\(72\)90053-3](https://doi.org/10.1016/0005-2736(72)90053-3)
 58. Kubrak OI, Rovenko BM, Husak VV et al (2012) Nickel induces hyperglycemia and glycogenolysis and affects the antioxidant system in liver and white muscle of goldfish *Carassius auratus* L. *Ecotoxicol Environ Saf* 80:231–237. <https://doi.org/10.1016/j.ecoenv.2012.03.006>
 59. Gupta S, Ahmad N, Husain MM, Srivastava RC (2000) Involvement of nitric oxide in nickel-induced hyperglycemia in rats. *Nitric Oxide Biol Chem* 4:129–138. <https://doi.org/10.1006/niox.2000.0278>
 60. Blackmore PF, Strickland WG, Bocckino SB, Exton JH (1986) Mechanism of hepatic glycogen synthase inactivation induced by Ca²⁺-mobilizing hormones. Studies using phospholipase C and phorbol myristate acetate. *Biochem J* 237:235–242. <https://doi.org/10.1042/bj2370235>
 61. Kraus-Friedmann N, Feng L (1996) The role of intracellular Ca²⁺ in the regulation of gluconeogenesis. *Metabolism* 45:389–403. [https://doi.org/10.1016/S0026-0495\(96\)90296-6](https://doi.org/10.1016/S0026-0495(96)90296-6)
 62. Barritt GJ, Litjens TL, Castro J et al (2009) Store-operated Ca²⁺ channels and microdomains of Ca²⁺ in liver cells. *Clin Exp Pharmacol Physiol* 36:77–83. <https://doi.org/10.1111/j.1440-1681.2008.05095.x>
 63. Soboloff J, Rothberg BS, Madesh M, Gill DL (2012) STIM proteins: dynamic calcium signal transducers. *Nat Rev Mol Cell Biol* 13:549–565. <https://doi.org/10.1038/nrm3414>
 64. Canaff L, Petit JL, Kisiel M et al (2001) Extracellular calcium-sensing receptor is expressed in rat hepatocytes. Coupling to intracellular calcium mobilization and stimulation of bile flow. *J Biol Chem* 276:4070–4079. <https://doi.org/10.1074/jbc.M009317200>
 65. Lytton J, Westlin M, Hanley MR (1991) Thapsigargin inhibits the sarcoplasmic or endoplasmic reticulum Ca-ATPase family of calcium pumps. *J Biol Chem* 266:17067–17071. [https://doi.org/10.1016/s0021-9258\(19\)47340-7](https://doi.org/10.1016/s0021-9258(19)47340-7)
 66. Zhang GH, Yamaguchi M, Kimura S et al (1990) Effects of heavy metal on rat liver microsomal Ca²⁺-ATPase and Ca²⁺-sequestering. Relation to SH groups. *J Biol Chem* 265:2184–2189. [https://doi.org/10.1016/s0021-9258\(19\)39959-4](https://doi.org/10.1016/s0021-9258(19)39959-4)
 67. Carafoli E (1994) Biogenesis: plasma membrane calcium ATPase: 15 years of work on the purified enzyme 1. *FASEB J* 8:993–1002. <https://doi.org/10.1096/fasebj.8.13.7926378>
 68. Prpic V, Green KC, Blackmore PF, Exton JH (1984) Vasopressin-, angiotensin II-, and α 1-adrenergic-induced inhibition of Ca²⁺ transport by rat liver plasma membrane vesicles. *J Biol Chem* 259:1382–1385. [https://doi.org/10.1016/s0021-9258\(17\)43414-4](https://doi.org/10.1016/s0021-9258(17)43414-4)
 69. Delgado-Coello B, Trejo R, Mas-Oliva J (2006) Is there a specific role for the plasma membrane Ca²⁺-ATPase in the hepatocyte? *Mol Cell Biochem* 285:1–15. <https://doi.org/10.1007/s11010-005-9060-z>
 70. Jiang JL, Yu MK, Chen ZN, Chan HC (2001) cGMP-regulated store-operated calcium entry in human hepatoma cells. *Cell Biol Int* 25:993–995. <https://doi.org/10.1006/cbir.2001.0751>
 71. Gregory RB, Rychkov G, Barritt GJ (2001) Does not involve inositol trisphosphate receptors. *Society* 290:285–290
 72. Gao H, Wang F, Wang W, Makarewich CA, Zhang H, Kubo H, Berretta RM, Barr LA, Molkentin JD (2012) Ca²⁺ influx through L-type Ca²⁺ channels and transient receptor potential channels

- activate pathological hypertrophy signalling. *J Mol Cell Cardiol* 53:657–667. <https://doi.org/10.1016/j.yjmcc.2012.08.005>
73. Hobai IA, Hancox JC, Levi AJ (2000) Inhibition by nickel of the L-type Ca channel in guinea pig ventricular myocytes and effect of internal cAMP. *Am J Physiol Hear Circ Physiol* 279:692–701. <https://doi.org/10.1152/ajpheart.2000.279.2.h692>
74. Wani SA, Khan LA, Basir SF (2018) Role of calcium channels and endothelial factors in nickel induced aortic hypercontraction in Wistar rats. *J Smooth Muscle Res* 54:71–82. <https://doi.org/10.1540/JSMR.54.71>
75. Anke M, Angelow L, Gleit M et al (1995) The biological importance of nickel in the food chain. *Fresenius J Anal Chem* 352:92–96. <https://doi.org/10.1007/BF00322304>
76. Grandjean P, Nielsen GD, Andersen O (1989). In: Maibach HI, Menné T (eds) Nickel and the skin: immunology and toxicology. CRC Press, Boca Raton
77. Varga I, Szebeni Á, Szoboszlai N, Kovács B (2005) Determination of trace elements in human liver biopsy samples by ICP-MS and TXRF: Hepatic steatosis and nickel accumulation. *Anal Bioanal Chem* 383:476–482. <https://doi.org/10.1007/s00216-005-0010-0>

Publisher's Note Springer Nature remains neutral with regard to jurisdictional claims in published maps and institutional affiliations.

Authors and Affiliations

Karina Sayuri Utsunomiya¹ · Lucas Jonatas da Silva¹ · Juliana Iwamoto¹ · Rodrigo Polimeni Constantin¹ · Eduardo Hideo Gilglioni¹ · Jorgete Constantin¹ · Adelar Bracht¹ · Ronald Petrus Johannes Oude Elferink² · Emy Luiza Ishii-Iwamoto¹ 

Karina Sayuri Utsunomiya
karina.utsunomiya@gmail.com

Lucas Jonatas da Silva
Lucas-jon@hotmail.com

Juliana Iwamoto
juh.iwamoto@gmail.com

Rodrigo Polimeni Constantin
rpconstantin@uem.br

Eduardo Hideo Gilglioni
gilglioni@hotmail.com

Jorgete Constantin
jconstantin@uem.br

Adelar Bracht
abracht@uem.br

Ronald Petrus Johannes Oude Elferink
r.p.oude-elferink@amc.uva.nl

¹ Laboratory of Biological Oxidations, Department of Biochemistry, State University of Maringá, Avenida Colombo 5790, Maringá, Paraná 87020900, Brazil

² Tytgat Institute for Liver and Intestinal Research, Academic Medical Center, University of Amsterdam, Amsterdam, The Netherlands